



Acute metal stress in *Populus tremula* x *P. alba* (717-1B4 genotype): leaf and cambial proteome changes induced by Cd²⁺

Thomas Durand, Kjell Sergeant, Sébastien Planchon, Sabine Carpin, Philippe Label, Domenico D. Morabito, Jean-François Hausman, Jenny Renaut

► To cite this version:

Thomas Durand, Kjell Sergeant, Sébastien Planchon, Sabine Carpin, Philippe Label, et al.. Acute metal stress in *Populus tremula* x *P. alba* (717-1B4 genotype): leaf and cambial proteome changes induced by Cd²⁺. *Proteomics*, 2010, 10 (3), pp.349-368. 10.1002/pmic.200900484 . hal-02666523

HAL Id: hal-02666523

<https://hal.inrae.fr/hal-02666523>

Submitted on 31 May 2020

HAL is a multi-disciplinary open access archive for the deposit and dissemination of scientific research documents, whether they are published or not. The documents may come from teaching and research institutions in France or abroad, or from public or private research centers.

L'archive ouverte pluridisciplinaire **HAL**, est destinée au dépôt et à la diffusion de documents scientifiques de niveau recherche, publiés ou non, émanant des établissements d'enseignement et de recherche français ou étrangers, des laboratoires publics ou privés.

1 **Acute metal stress in *Populus tremula x P. alba* (717-1B4 genotype): leaf
2 and cambial proteome changes induced by Cd²⁺**

3
4 Durand, Thomas C₂^{abcd}; Sergeant, Kjell^a; Planchon, Sébastien^a; Carpin, Sabine^{bc}; Label,
5 Philippe^d; Morabito, Domenico^{bc}; Hausman, Jean-François^a; Renaut, Jenny^{a*}

6
7 ^a CRP-Gabriel Lippmann, 41 rue du Brill, L-4422 Belvaux, GD, Luxembourg. Department
8 Environment and Agro-biotechnologies.

9 ^b Université d'Orléans, UFR-Faculté des Sciences, Laboratoire de Biologie des Ligneux et des
10 Grandes Cultures, UPRES EA 1207, rue de Chartres, BP 6759, 45067 Orléans Cedex 02, France.

11 ^c INRA, USC2030 'Arbres et Réponses aux Contraintes Hydrique et Environnementales'
12 (ARCHE), 45067 Orléans, France.

13 ^d Institut National de la Recherche Agronomique, CS40001 Ardon, 2163 Avenue de la
14 pomme de pin, 45075 Orléans CEDEX 2, France.

15 * To whom correspondence should be addressed. E-mail: renaut@lippmann.lu

16
17 **Acknowledgment :**

18 The authors are grateful to Thomas Udelhoven for his helpful expertise in statistics and
19 to Vanessa Caruso for English correction.

20 Thomas Durand was supported by a PhD fellowship of the Luxembourg Ministry of
21 Culture, Higher Education and Research (BFR 05/094) and a National funds for Research
22 grant (AFR)

23
24
25 Keywords : Cadmium, Cambium, Fluorescence two-dimensional difference gel
26 electrophoresis, Mass spectrometry, Metal stress, Phytoremediation.

27
28 Abbreviations: DAP: DNA-binding Aspartyl Protease / PRP: proline-rich protein / PSII :
29 Photosystem 2.

30 **ABSTRACT**

31 The comprehension of metal homeostasis in plants requires the identification of
32 molecular markers linked to stress tolerance. Proteomic changes in leaves and cambial
33 zone of *Populus tremula x P. alba* (717-1B4 genotype) were analysed after 61 days of
34 exposure to Cd 360 mg.kg⁻¹ soil dry weight in pot-soil cultures.

35 The treatment led to an acute Cd stress with a reduction of growth and photosynthesis. Cd
36 stress induced changes in the display of 120 spots for leaf tissue and 153 spots for the
37 cambial zone. It involved a reduced photosynthesis, resulting in a profound
38 reorganisation of carbon and carbohydrate metabolisms in both tissues. Cambial cells
39 underwent stress from the Cd actually present inside the tissue but also a deprivation of
40 photosynthates caused by leaf stress. An important tissue specificity of the response was
41 observed, according to the differences in cell structures and functions.

42 **INTRODUCTION**

43
44 Cadmium (Cd) is regarded as one of the most toxic heavy metals, responsible for human
45 and plant diseases^[1,2]. When plant physiology is affected by Cd stress, symptoms are
46 generally chlorosis, necrosis, leaf rolling or drying and growth inhibition^[3]. Cd toxicity
47 arises notably from competition with Zn for binding sites in biomolecules, e.g enzymes
48 or carriers^[4,5].

49 Since a few years *Salicaceae* (e.g. willows and poplars) have emerged as promising
50 candidates in the search for convenient species to achieve phytoremediation of polluted
51 sites^[6]. Indeed, poplar, whose small genome is now completely sequenced, is a suitable
52 model plant to support molecular studies on stress response's^[7,8]. Poplar is reported to be
53 able to thrive despite metal contamination, and to accumulate metals, especially cadmium
54 ^[9]. Being a perennial species poplar furthermore allows the opportunity to shape an ideal
55 phytoremediator. Year after year accumulation of metals in harvestable woody tissues
56 provides a convenient means of soil clean up combined with the potential of energy
57 production. As a model-tree species poplar can also be used to study the metabolic
58 mechanisms of metal uptake and tolerance in woody species.

59 The plant responses to metal stress are mediated through modifications in gene
60 expression and protein levels. Proteins that participate in metal tolerance response are
61 reported to be involved in the induction of transcription factors, in the protection or
62 restoration of macromolecules and in detoxification activities^[10].

63 Metal homeostasis and detoxification are known to be partly constitutive^[2], but
64 inducible parts of these processes can be explored by a proteomic approach. Although
65 proteomic research has been conducted on the effects of metals on plants, e.g. on the
66 response to Cd in roots of *Oryza sativa*^[11], in cell cultures of *Arabidopsis thaliana*^[12], in
67 leaves of *Spinacia oleracea*^[13] or in roots and shoots of *Thlaspi caerulescens*^[14], a
68 recent review by Ahsan, Renaut & Komatsu^[15] deplored the limited proteomic
69 investigations on this topic, especially for long-term exposition. Kieffer *et al.*^[16,17]
70 recently reported proteome changes in leaves of poplar exposed to Cd up to 56 days
71 under hydroponic conditions.

72 The comprehension of the tolerance of plants to environmental constraints requires a
73 profound description of the acting molecules during the response. Typically, a constraint

POSTPRINT :

**Version définitive du manuscrit publié dans / Final version of the manuscript published in :
Proteomics, 2010, 10(3), 349-368**

74 will evoke a stress perception and a stress signalization leading to damage avoidance and
75 repair. For each step of the plant response, some of the involved molecules belong to a
76 generic pattern of response to all biotic/abiotic stresses, while others can be related to one
77 specific stressor. Current research mainly deals with molecules involved in the response
78 to a range of diverse constraining conditions, *e.g.* chaperones, antioxidants, proline, plant
79 growth regulators, etc. [18,19,20,21]. These molecules are responsible for the General
80 Adaptation Syndrome (GAS), initially formulated by Selye in 1951 [22,23]. However, one
81 type of stress will not equally affect the dissimilar tissues within an individual. Published
82 proteomic studies of plant stress most often concern leaf or root tissues. This is graspable
83 considering that the photosynthetic apparatus is often affected by heavy metal toxicity
84 [24], while roots are directly exposed to the contaminated environment. Yet, other tissues
85 can be considered to complement the analysis. In woody species the cambium activity
86 determines the secondary growth that represents a physical support for the extended
87 primary growth of the tree. It also shapes the structure of conductor tissues –number and
88 size of wood vessels and fibers, cellular composition of phloem. Cambium activity
89 eventually influences the production of biomass wherein heavy metals can be
90 accumulated. Despite its importance, the cambium response remains scarcely questioned.
91 Available studies on the cambial tissue generally focus on developmental questions [*e.g.*
92 25,26] and few deal with biotic stress [27] or abiotic stress [28].

93 A proteomics approach on the responses of plants during exposure to pollutants, *in*
94 *casu* cadmium, will point out the molecular actors supporting metal intake and also give
95 information about stress-related responses in different tissues. This knowledge will allow
96 the selection or the design of plants that prevent deleterious metal accumulation along the
97 food chain (like cadmium), or, on the contrary, crops that could solve problems of human
98 essential metal deficiencies.

99 In this study, young poplar plants were exposed to a soil contaminated by the addition
100 of 360 mg Cd.kg⁻¹ soil dry weight (SDW), corresponding to a total amount of 1 mmol of
101 metal per liter of soil. Ecophysiological parameters were monitored all along the 61 days
102 of exposure to characterise the physiological state of the plant. Metal distribution in the
103 tree was also determined. A subsequent proteome analysis on leaf and cambial tissues

POSTPRINT :

Version définitive du manuscrit publié dans / Final version of the manuscript published in :
Proteomics, 2010, 10(3), 349-368

104 illustrated the acute stress endured by Cd and its strong effect on photosynthesis and
105 carbon metabolism.

106

107 **2. MATERIAL AND METHODS**

108

109 **2.1. Plant material and metal constraints**

110 Pot-grown *Populus tremula L. x P. alba L.* (*Populus x canescens* (Aiton) Smith)
111 genotype INRA 717-1B4 were obtained as previously described in Durand *et al.* (2009,
112 submitted). Once rooted and 3 months old, poplar plants were pruned and transplanted
113 from 0.3 L pots to 10 L pots filled with a sand - peat moss soil mixture (25:75, v/v, pH
114 6.9). Cadmium was incorporated in the 10 L soils by uniformly hand mixing.

115 Control soil contained no detectable cadmium. Cadmium contaminated soil contained
116 360 mg Cd.kg⁻¹ SDW. Soil solution concentrations were determined from 100 g of fresh
117 soil after 20 min of centrifugation at 10,000 g. The supernatant was collected for
118 quantification using a Jobin-Yvon® HR-ICP-AES, as described in [29]. Soil solution of
119 metal-exposed plants contained 20.8 µM Cd²⁺.

120 Plants were grown in culture chamber at 21°C, 70% of relative humidity, and with an
121 irradiance of 1000 µmol.m⁻².s⁻¹ provided during 16 h per day. After 61 days of metal
122 exposure, leaf and woody tissues were collected and frozen in liquid nitrogen and stored
123 at -80°C until protein extraction.

124

125 **2.2. Protein extraction and sample preparation**

126 Four biological replicates corresponding each one to individual plants were used.
127 Leaf proteins were extracted starting from 500 mg of fresh weight collected from the
128 three last fully expanded leaves of one plant. After lyophilisation of the cutting, the bark
129 was excised. The cambial zone was then collected by softly scratching the inner face of
130 the bark with a scalpel. Proteins from the cambial zone were extracted from
131 approximately 60 mg of dry tissue of each replicate. Tissues were ground in liquid
132 nitrogen. Proteins were extracted using the TCA-acetone precipitation method described
133 by Damerval *et al* [30]. Resolubilisation of the precipitated proteins was carried out in a
134 lysis buffer (7M urea, 2M thiourea, 4% w/v 3-[(3-cholamidopropyl)-dimethylammonio]-

POSTPRINT :

**Version définitive du manuscrit publié dans / Final version of the manuscript published in :
Proteomics, 2010, 10(3), 349-368**

135 1-propane sulfonate (CHAPS), 30 mM Tris pH 8.5. The protein extracts were quantified
136 using a quantification kit (2D-Quant Kit, GE healthcare) with bovine serum albumin as
137 standard.

138 After quantification, proteins were labelled by mixing 240 pmol of fluorochromes
139 (CyDyes™, GE Healthcare) with 30 µg proteins. For each gel, Cy3 and Cy5 were used
140 for control or treated samples; Cy2 was used for the internal standard consisting of a mix
141 of equal amounts of each sample. A dye swap was used between Cy3 and Cy5 to avoid
142 problems associated with preferential labelling.

143

144 **2.3. Protein separation and relative quantification (2-D DIGE)**

145 Bidimensional electrophoresis was carried out as described in Bohler *et al.* [31], with
146 slight modifications. The isoelectric focusing was carried out on pH 3-10 IPG-strips (24
147 cm, non linear gradient; GE Healthcare, Little Chalfont, UK) using the IPGphor system
148 from GE Healthcare. Protein samples were cup loaded. The migration was performed at
149 20°C (\leq 50 µA, 60V for 2 h; gradient from 60 V to 1,000 V for 3h ; hold 1,000 for 1h,
150 gradient from 1,000 to 8,000 for 3 h; hold 8,000 V until 85,000 V.h). Strips were then
151 stored at -20°C.

152 Prior to second dimension migration, the strips were equilibrated. During
153 equilibration, proteins were reduced by 1% DTT for 15 min and then alkylated by 2.5%
154 (w/v) iodoacetamide for 15 min. The SDS-PAGE was carried out on 12.5% (w/v) of
155 acrylamide-bisacrylamide (37.5/1) gels. Proteins were separated by applying 1.5 W per
156 gel for 20 min, and then 2 W per gel until the migration front reached the end of the gel.
157 After migration and fixing of proteins in the gel, images were captured using a Typhoon
158 Variable Mode Imager 9400 (GE Healthcare).

159 DeCyder v.6.05.11 software (GE Healthcare) was used to determine differentially
160 expressed proteins with a variation factor of at least 1.3 in abundance (up and down) and
161 a significant Student t-test score ($p < 0.05$). The automated matching was manually
162 confirmed for all the spots that were selected for identification, and that are further
163 discussed. Spots were picked from the gel and digested by trypsin for 6 h at 37°C using
164 an Ettan Dalt Spot Handling Workstation (GE Healthcare) before acquisition of peptide

POSTPRINT :

**Version définitive du manuscrit publié dans / Final version of the manuscript published in :
Proteomics, 2010, 10(3), 349-368**

165 mass spectra with a MALDI-TOF-TOF analyser (4800 Applied Biosystems, Foster City,
166 CA, USA).

167

168 **2.4. Protein identification.**

169 As the poplar genome is not yet completely annotated and many sequences were only
170 available as ESTs, protein identification was mainly done using the EST-database on an
171 in-house mascot platform. The NCBI poplar EST database used in this study contains
172 419,944 poplar sequences and was downloaded from the NCBI database on 06/11/2009.
173 MS and MS/MS data were also submitted for analysis with a viridiplantae protein
174 database downloaded on 02/17/2009 and containing 1,214,000 sequences. All searches
175 were carried out using a mass window of 100 ppm for the precursor and 0.5 Da for the
176 MS/MS fragments. Up to 2 trypsin miscleavages were accepted. The search parameters
177 allowed for carbamidomethylation of cysteine, oxidation of methionine as well as
178 oxidation of tryptophan to kynurenine and double oxidation of tryptophan to N-
179 formylkynurenine. During automatic interrogation of databases, the MASCOT score cut-
180 off was 77 for NCBI and 65 for EST interrogations. Because all spectra and
181 identifications were manually verified, peptide scores were considered even below the
182 cut-off values for peptide scores. Identifications were validated manually with at least
183 two identified peptides at disparate sites within a protein with a score above homology.

184 Percentage of sequence coverage was given in Tables 1 & 2. Since EST's generally do
185 not represent an entire protein sequence, the authors would like to remark that this value
186 has little significance when identifications were done on EST sequences. Grouping of
187 proteins in biological process was done accordingly to KEGG and Uniprot databases
188 (<http://www.genome.jp/kegg> ; <http://www.uniprot.org/>). The functions of some proteins
189 were enlightened by the use of InterPro^[32] (<http://www.ebi.ac.uk/interpro/>) which
190 consists in blasting the amino sequences to the integrated resources of several databases
191 like PANTHER, PROSITE and Gene3D.

192 In leaf and cambial proteomes, respectively in 2 and 7 spots, more than 1 protein was
193 identified, since this prevents any interpretation about the actual abundance of change in
194 them, biological discussion was not done on these proteins. They are nonetheless
195 presented at the end of Tables 1 & 2.

POSTPRINT :

Version définitive du manuscrit publié dans / Final version of the manuscript published in :
Proteomics, 2010, 10(3), 349-368

196

197 **2.5. Statistics**

198 Statistical analysis was carried out with 4 biological replicates. The variable used for
199 comparison was the log10 of standardized volume of protein spots in the gels. A Student
200 t-test analysis was carried out in the DeCyder software. The results based on the log10 of
201 standardised volume of protein spots in the gels were provided by the DeCyder software
202 by Student t-test analysis. A false discovery rate correction was applied in the software .
203

204 **3. RESULTS**205 **3.1. Leaf proteome profiles.**

206 The 2D electrophoretic leaf pattern presented 1,023 spots (Figure 1). Among them,
207 120 spots exhibited a significant absolute variation greater than 1.3-fold between control
208 and treated conditions ($p < 0.05$). The Cd treatment resulted in an increased abundance for
209 40 protein spots, and a decreased abundance for 80 protein spots. The MS analysis of
210 these spots resulted in the confident identification of 103 proteins, of which 2 were a mix
211 of at least two proteins (Table 1).

212 Briefly, the significant changes in protein abundance occurred in the following
213 functions (Table 4): photosynthesis (44 protein spots), carbon and carbohydrate
214 metabolism (21), energy metabolism (9), proteins metabolism, catabolism and folding
215 (9), citrate cycle (5), oxidoreduction (6) and glutathione metabolism (2). Other functions
216 that were influenced include an inositol-3-phosphate synthase (spot 572), a potassium
217 channel beta subunit (spot 1300), an auxin-binding protein ABP19a precursor (spot
218 1756), an alpha tubilin (spot 1192) and a translation elongation factor (spot 225).

219 When the same protein was identified in several spots, as is for instance the case for
220 Ferredoxin-NADP oxidoreductase in spot 1340, 1332, 1342, 1338, 1365 and 1359, the
221 MS spectra were compared in order to find posttranslational regulatory events. For none
222 of the proteins for which this comparison was done supplementary information was
223 obtained.

224

225 **3.2. Cambium proteome profiles.**

POSTPRINT :

**Version définitive du manuscrit publié dans / Final version of the manuscript published in :
Proteomics, 2010, 10(3), 349-368**

226 The 2D electrophoretic cambium pattern presented 1,144 spots (Figure 2). Among
227 them, 153 exhibited a significant absolute variation greater than 1.3-fold between control
228 and treated conditions ($p<0.05$). Compared to control conditions, the Cd treatment
229 resulted in the increased intensity of 47 proteins spots, while 106 spots were less intense.
230 The MS analysis of the differential spots resulted in the confident identification of the
231 proteins in 108 spots among which 7 presented a co-migration of more than 1 protein
232 (Table 2). The remaining 30% of the selected spots are still unidentified because of the
233 weak intensity of the spectra resulting from faintly stained spots. Furthermore, few ESTs
234 corresponding to cambial tissue are available.

235 Among the cambial proteins, 8 spots were identified as ‘aspartyl protease family
236 protein’ (spots number 398, 913, 996, 1140, 1146, 1157, 1488 and 1495), and 8 others as
237 ‘nucleoid DNA-binding protein cnd41-like protein’ (spots 1106, 1115, 1142, 1148, 1149,
238 1169, 1177 and 1206). As these two groups of proteins exhibited common MS/MS
239 peptides, like ‘TYTIVFDGAKER’ or “ITASDYIVNVGIGTPKK”, an InterProscan
240 interrogation was realised. Both of them designated proteins that possess a chloroplast
241 nucleoid DNA-binding domain as well as an aspartyl peptidase domain. Therefore, they
242 were gathered in the Tables 2 and 4 under the label “DNA-binding aspartyl peptidase”.

243 Briefly, the significant changes in protein abundance specifically induced by Cd
244 treatment occurred in the following functions (Table 4): carbon and carbohydrate
245 metabolisms (22), cytoskeleton & cell wall (18), DNA binding peptidase (16), protein
246 metabolism, catabolism and folding (16), transcription and translation factors (8),
247 antioxidation and stress-related functions (6), lipid metabolism (5), the citrate cycle (3),
248 and others functions among which a cupin family protein (spot 1179), two beta-subunits
249 of K⁺ channels (spot 1375, 1376) and two putative adenosine kinase (spots 1129 and
250 1135) were down-regulated in Cd-treated poplars whereas a Phi-1 (spot 1492), an
251 eukaryotic initiation factor 4A (spot 880) and a DEAD box RNA helicase (spot 877) were
252 up-regulated in Cd-treated poplars.

253

254

255 **4. Discussion.**

POSTPRINT :

Version définitive du manuscrit publié dans / Final version of the manuscript published in :
Proteomics, 2010, 10(3), 349-368

256 Young *Populus tremula x P. alba* 717-1B4 genotype plants were exposed to 360
257 mg Cd.kg⁻¹ SDW, this resulted a in soil solution concentrations of 20.8 µM Cd²⁺. An in-
258 soil experiment permitted to follow the dynamic ion partition between soil and plant,
259 which may be a determining factor in the response of the plant^[33,34]. The study aimed at
260 analyzing tissues that have grown and developed under metal constraints. This allowed to
261 focus on distal equilibrium rather than on the alarm phase of stress. Thus, control and
262 stressed plants were compared after 61 days of cadmium exposure.

263 The Cd treatment resulted in a Cd accumulation in the leaves (84 mg Cd.kg⁻¹) and in
264 the cambial zone (123 mg Cd.kg⁻¹). The treatment drastically reduced the growth of the
265 plants. Net photosynthesis and stomatal conductance were inhibited. Increases in the
266 content of K⁺, Ca²⁺, Mg²⁺ and Zn²⁺ in tissues, especially in leaves, were observed. These
267 results are summarized in the Table 3 (adapted from^[29]). The physiological data
268 demonstrate that Cd²⁺ triggered an acute stress in poplar plants from which ensues
269 important changes in leaf and cambial proteome (Figures 1 & 2).

270

271 **4.1. Leaf proteome response to Cd**

272 The proteomic data gave two levels of information that can hardly be distinguished.
273 Some changes occurred as a consequence of the stress endured, while others constitute
274 the concrete and active response of the plant defense system. The Impact Factor (IF) on
275 protein abundance was calculated as the ratio of the volume of protein spots between
276 treated and control conditions.

277 In leaf and cambial tissues the cadmium stress mainly affected the carbon metabolism.
278 In the leaf, negative IF was salient on the carbon fixation, especially on ribulose-1,5-
279 bisphosphate carboxylase/oxygenase (RuBisCO) and RuBisCO activase. Other proteins
280 involved in the Calvin Cycle were also affected (spots 284, 1116, 1120, 1124, 1127,
281 1566, 1571). Additionally 3 out of 4 spots wherein carbonic anhydrase was identified
282 decreased in intensity in Cd-treated plants (spots 1592, 1598, 1616, 1660).

283 These data are consistent with our previous results, which describe the inhibition of
284 CO₂ assimilation under Cd stress, which was mainly unrelated to stomata closure^[29]. The
285 literature diversely reports on the stomatal response to Cd stress, although stomata
286 closure is often regarded as a typical response^[35,36,37]. Shi and Cai^[38] observed a Cd-

POSTPRINT :

Version définitive du manuscrit publié dans / Final version of the manuscript published in :
Proteomics, 2010, 10(3), 349-368

287 induced xerophytes-like leaf morphology with more frequent but smaller stomata,
288 accompanied by a reduced stomatal conductance in peanut (*Arachis hypogaea*). On the
289 contrary Zhu, Macfie & Ding [39] reported that Cd-exposed *Brassica juncea* showed
290 fewer although larger stomata. In both cases, the reduced stomatal aperture only partly
291 explained the decreased photosynthetic activity.

292 Whatever the stomatal response, the Cd toxicity mostly arises through other processes
293 than gas exchange. In this study, the strongest negative influence of Cd on spot intensity
294 was observed for photosynthesis-related proteins. This reduced intensity was particularly
295 observed for proteins implied in the electron transport: chlorophyll a/b binding proteins
296 (10 spots down regulated, with IF from -2.08, spot 1584, to -11.02, spot 1517, Table 1),
297 Oxygen Evolving Enhancer (5OEE1 spots and 5 OEE2 spots, *i.e* 33 kDa and 23 kDa
298 subunits respectively, all down regulated, with IF from -2.75, spot 1456, to -7.03, spot
299 1441) and ferredoxin-NADP oxidoreductase (5 spots down-regulated, *e.g.* spot 1340, 2
300 other up regulated, *e.g.* spot 1338). The decrease of the photosynthetic activity, inferred
301 from the diminished CO₂ assimilation (Table 4) is further suggested by the drop in
302 abundance of a FtsH protease 8 which contributes to the turnover of the Photosystem II
303 D1 protein [40]. These results incline to show a major impact on proteins of the PSII,
304 which is contradictory with a recent study on spinach where PSI was described as more
305 sensitive to Cd²⁺ [4]. Among the 5 ATPase spots differentially expressed, 3 were down-
306 regulated (spots 620, 632 and 633), all of them chloroplastic ATPase. The 2 up-regulated
307 ATPase are localized in the mitochondrion, according to the databases (spots 594 & 599).
308 This suggests that photosynthetic processes are inhibited by Cd stress, while respiration,
309 on the contrary, is promoted. Supporting the latter, the increase in quantity of a succinate
310 dehydrogenase spot was recorded (spot 418). This enzyme takes part in the mitochondrial
311 respiratory chain. Changes in the abundance of TCA cycle enzymes, increased
312 accumulation of citrate synthase (spots 902, 903) and decreased abundance of malate
313 dehydrogenase (spots 1200, 1316), do not result in a consensus on how the respiration is
314 affected during Cd stress, but confirm that there is an effect. Consistently with an
315 increased respiration concomitant to a suppressed photosynthesis, an induction of
316 glycolysis-involved enzymes was observed: UDP-glucose pyrophosphorylase (spot 597),
317 glycosyl hydrolase family 38 protein (spot 553), 3-phosphoglycerate kinase (spot 1051).

POSTPRINT :

Version définitive du manuscrit publié dans / Final version of the manuscript published in :
Proteomics, 2010, 10(3), 349-368

318 Such a relation between suppressed photosynthesis and stimulated respiration from
319 glucose catabolism in leaves was previously reported under Cd stress^[41], ozone stress
320^[42], drought and heat stress^[43].

321 Beside the inhibition of the carbon and carbohydrate metabolism, the analysis of the
322 leaf proteome gives clues of an inhibited protein metabolism. The proteome change
323 patterns suggest reduced protein synthesis (aminomethyltransferase, spot 1290, and
324 translation elongation factor EF-G, spot 225, inhibited), reduced protein transport (2
325 nascent polypeptide associated complex alpha chain inhibited, spots 1518 and 1752) and
326 reduced protein degradation (proteasome subunit PRGB inhibited, spot 1678).
327 Modifications of protein processes are often a way to avoid damages or to ensure
328 replacement of damaged molecules. Nevertheless, in this case, the observed changes
329 rather resulted from supply shortage due to a reduced primary metabolism in a leaf tissue
330 whose growth was heavily inhibited. Interestingly the strongest IF in the leaf proteome
331 was that of a phosphoglycerate dehydrogenase (+ 36.7, spot 548). This enzyme, involved
332 in the synthesis of several amino acids like glycine, serine or threonine, might also play a
333 role in the glutathione production.

334 Changes in the glutathione metabolism are widely reported to be part of most plant
335 response to Cd^[44,45,46,16]. Direct measurement of this metabolism was not performed, but
336 indirect hints may nonetheless be considered. Two glutathione-S-transferase were up-
337 regulated (spot 1659 and 1667), as was a formate dehydrogenase (spot 1061); its role is
338 the production of reducing power (NADH). A GDP-mannose 3,5-epimerase/ NAD
339 binding protein (spot 936), implied in the ascorbate synthesis, was up-regulated.
340 Ascorbate and glutathione are coordinated in the cell by the Halliwell-Asada Cycle.
341 Interestingly, the strongly induced (IF+16.7, spot 1637) 1-cys peroxiredoxin is a
342 bifunctional enzyme with phospholipase A2 and glutathione peroxidase activities^[47].
343 This denotes, as expected, an impact of Cd on the redox status of the cell, as confirmed
344 by the abundance of changes in a type 2 peroxiredoxin (IF-2.09, spot 1821). This impact
345 could explain the changes of protein folding-involved HSP 70 (IF-1.59, spot 1011, and
346 +1.6, spot 357) and chloroplast chaperonin 21 (IF-2.23, spot 1635). This could also
347 indicate an impact of Cd on the integrity of membranes, since one inositol-3-phosphate
348 synthase (IF-1.99, spot 572) is negatively affected. These changes, as well as the decrease

POSTPRINT :

**Version définitive du manuscrit publié dans / Final version of the manuscript published in :
Proteomics, 2010, 10(3), 349-368**

349 of an alpha tubulin (IF-2.94, spot 1192) might also be connected to the leaf growth
350 inhibition in spite of a sampling realized on fully expanded leaves. Indeed, the Cd-treated
351 sampled leaves presented a significantly smaller size than control.

352 A stimulated potassium channel beta subunit (IF+1.6, spot 1300) converged with
353 previous results showing a significant alteration of potassium homeostasis under Cd
354 stress [29]. The $[K^+]_{leaves}$ increased 2.3-fold compared to control plants (Table 4). In the
355 cambial zone, on the contrary, two beta-subunit of K^+ channels decreased in quantity;
356 linked to the 48% reduced $[K^+]_{cutting}$. Only few reports on the regulation of mineral
357 homeostasis under Cd stress are available in the literature. A recently published paper
358 indicated no change in K^+ and Mg^{2+} content in leaves of Cd-tolerant mungbean (*Vigna*
359 *radiata*) under Cd exposure [48]. To our knowledge neither the mobilization of K^+ in
360 leaves in response to Cd, nor the implication of a potassium channel were reported so far.

361 It is not surprising that Cd disturbs metal homeostasis, even if proteomic data give
362 little indication on it. For instance the 2-fold increase of $[Mg^{2+}]_{leaves}$ (Table 4) can be
363 linked to the instability of photosynthesis proteins like the rubisco activase that often
364 have Mg^{2+} as cofactor. The increased $[Mg^{2+}]$ could be needed to compete with the toxic
365 Cd²⁺ in order to reduce proteins misfolding and inactivation.

366 The comparison of these results with those from a previous hydroponic poplar
367 exposure to Cd [17,16] exhibits some common traits that were underlined above, but also
368 some differences. Hydroponic and soil conditions partly affect plant physiology in
369 differential ways, notably metal bioavailability. This could account for a part of these
370 differences in the proteomic response.

371 For instance, a chitinase (spot 1552) was the sole identified pathogenesis-related (PR)
372 protein affected by Cd in leaves in this study, whereas this type of proteins was shown to
373 accumulate, especially on the long term (day 56), in Kieffer's articles [17,16]. Cd-
374 responsive proteins implied in oxidoreduction were more numerous in leaf than in
375 cambial zone, with an overall negative impact of the stress. When comparing with
376 exposure to Cd in a hydroponic system, it appears that these protein functions are more
377 responsive on a shorter time scale (7-14 days) than on 56 days.

378

379 **4.2. Cambial proteome response to Cd**

POSTPRINT :

**Version définitive du manuscrit publié dans / Final version of the manuscript published in :
Proteomics, 2010, 10(3), 349-368**

As in leaf, the carbon metabolism is the principal biological process altered in cambial proteome in response to Cd. The differentially expressed proteins are partly corresponding to the same functions as in leaf (e.g. 3 malate dehydrogenase, spots 1268, 1290, 1336 ; 1 triosphosphate isomerase, spot 759, and 1 UDP glucose pyrophosphorylase, spot 752, all of them were inhibited in the cambial zone). In addition to these proteins, the overall changes linked with carbohydrate metabolism indicate an impact on glycolysis and glycogenesis. Five spots of enolase were down-regulated (e.g. spot 784, 798, 800, 802, 816). Three spots of UDP glucose dehydrogenase (spots 744, 752, 809), one phosphofructokinase family protein (spot 851), one 2,3-bisphosphoglycerate-independent phosphoglycerate mutase (spot 526) and one fructokinase (spot 1202) decreased, whereas 2 alcohol dehydrogenase (spots 1069 & 1070) increased in quantity. Two spots of alpha-D-xylosidase (spots 288 & 1892) were more intensively stained. This enzyme is reported to be analogous to alpha glucosidase [49]. Hence the overall carbohydrate metabolism was reduced.

In cambial zone as in the leaf, the great disturbance in the carbohydrate metabolism is obviously a distal consequence of Cd stress. A previous work on poplar response to Cd showed changes in sugars content [17]. Such changes, beyond stress symptomatology, probably take part in the sensing and signaling of the constraint [50] even if the alarm phase is very likely to have ceased before day 61. Most sugars are known to improve osmoprotection during stress ; this is a role they could also play in the metal stress [51].

The protein metabolism is the second biological process influenced by Cd stress in the cambial zone. Protein synthesis was reduced, as attested by the decreased abundance of 4 spots containing methionine synthase (spots 381, 383, 385, 391), 3 spots containing S-adenosylmethionine synthetase (spots 881, 885, 891), an O-acetylserine (thiol)lyase (spot 1240), and a 60S acidic ribosomal protein P0 (spot 1302). There was also one differentially displayed spot of eukaryotic initiation factor 4A (spot 902), and 3 others of elongation factor 1- γ (spots 332, 892, 911). One calreticulin-1 (spot 715) and 3 protein disulfide-isomerase precursors (spots 537, 541, 1161), related to protein folding exhibited a reduced abundance. Proteolysis was also affected, with the decreased abundance of two proteasome subunits (spots 896 & 1555) and of a Zn-dependent leucine aminopeptidase (spot 796), and also 2 more abundant alpha-mannosidase (spots 390 and 433) involved in

POSTPRINT :

**Version définitive du manuscrit publié dans / Final version of the manuscript published in :
Proteomics, 2010, 10(3), 349-368**

411 the vacuolar degradation of glycoproteins. So protein metabolism, folding and catabolism
412 appeared to be impaired by Cd treatment.

413 Cd-stress also induced changes in proteins involved in cell structure and cell wall,
414 hence related to the growth function of the meristem. Two spots of rhamnose
415 biosynthesis 1 (spots 480, 487) were less abundant, one was more abundant (spot 481);
416 this enzyme participates to the production of rhamnose, an important constituent of the
417 cell wall [52]. Also in relation with cell wall synthesis, 3 spots of phenylcoumaran
418 benzylic ether reductase dropped in intensity (spots 1319, 1323, 1340). This enzyme is
419 strongly associated with phenylpropanoid biosynthesis in lignifying cells of poplar [53].
420 One cinnamoyl-CoA reductase (spot 1324), involved in the synthesis of lignin and a
421 leucine rich repeat protein (spot 1317), also implied in cell wall synthesis [54] decreased in
422 amount. Two spots of reversibly glycosylated polypeptides (spots 1168 & 1187) dropped
423 in intensity; these proteins, supposed to be plasmodesmata-associated [55] are linked to
424 cell elongation and related to cell wall formation, even if their precise role in the cell
425 remains unsolved [56]. Consistently with an inhibition of growth, 2 spots containing
426 adenosine kinase (spots 1129 & 1135), implied in nucleic acid synthesis, exhibited lower
427 content.

428 According to Garnier *et al.* [57], Cd cytotoxicity arises notably through three waves of
429 oxidative stress in tobacco cells. In the present study, in cambial tissue as it was the case
430 in leaves, the redox balance appears to be disturbed. A class III peroxidase (spot 1137)
431 was more abundant. Two 6-phosphogluconate dehydrogenase family proteins (spots 908
432 & 909), involved in the glutathione metabolism, decreased in amount, whereas a
433 glutathione-S-transferase was more abundant (spot 1657). The lower accumulation of a
434 glutamate decarboxylase (spot 796) was observed, but a putative leucine aminopeptidase
435 was identified in the same spot, preventing any interpretation concerning this calmodulin-
436 binding protein that produces GABA (γ -aminobutyric acid).

437

438 The suppression of cytoskeletal-linked proteins such as α and β chain tubulin (7 spots
439 down regulated, e.g. spot 772) or actin (spots 977, 990) in cadmium exposed poplar
440 confirms the main role of cambium as an actively growing tissue, and the different
441 growth rates between control and exposed plants. Two spots of glycine-rich RNA-

POSTPRINT :

**Version définitive du manuscrit publié dans / Final version of the manuscript published in :
Proteomics, 2010, 10(3), 349-368**

442 binding protein (spots 1836 & 1838) appeared differentially expressed. This protein
443 family of post-transcriptional regulators has been showed playing a role in cold
444 acclimation of *Arabidopsis* [58]. Cd induced antagonistic changes in 2 putative proline-
445 rich protein (PRP) (spots 926 & 1057). These cell wall structural proteins are reported to
446 accumulate under water deficit in *Phaseolus vulgaris* cells [59]. When the respective EST
447 sequences for these spots were used in BLAST analysis, the results indicated that they
448 contain a "GDSL" motif close to the N-terminus. In addition 2 GDSL-motif
449 lipase/hydrolase family protein spots decreased in amount (spots 572 & 576). These
450 proteins could have a role in the degradation of complex polysaccharides [60,61]. The
451 GDSL family has been repeatedly reported to be implied in diverse stress responses [62].
452 Among the 159 Cd-affected proteins in the cambial zone, 7 have Zn as cofactor (spots
453 796, 1069, 1070, 537, 541, 1161, 715), and 4 others potentially binds Zn (1302, 1836,
454 1838, 1179). All of them, except the 2 alcohol dehydrogenase and one of the 2 glycine-
455 rich RNA-binding protein were reduced in quantity. In the leaf proteome 7 out of 114
456 identified Cd-affected proteins needs Zn for functioning (spots : 435, 1548, 1563, 1592,
457 1598, 1616, 1660). When compared to the counted 2367 Zn-related proteins of *A.
458 thaliana* [63], out of 159,162 entries in database for this species (according to "porgn:
459 txid3702" request on <http://www.ncbi.nlm.nih.gov>), the present proportion of Zn-related
460 proteins affected by Cd stress did not clearly suggest a particular and quantitative
461 involvement of them in the response.

462 The quantitatively most prominent information about cambial proteome response
463 concerns plastidial DNA-binding aspartyl peptidase (DAP). Increased abundance in
464 proteolytic enzymes has already been observed in studies on poplar leaves and roots
465 under Cd exposure, but no influence on the abundance of DAP in this study under
466 hydroponic condition was observed [16]. Sixteen DAP spots showed a differential
467 expression under Cd stress (e.g. spot 1140), 12 were up-regulated, with IF up to 5.05
468 (spot 398). Kato *et al.* [64] reported a link between nucleoid DNA-binding protein cnd41-
469 like protein – which is a DAP – and the degradation of RuBisCO in tobacco leaves during
470 senescence. Yet no differences in the expression of DAP were observed in the leaves of
471 poplar plants. Although some cambium cells express photosynthetic genes, including at
472 least RuBisCO subunits [65], it seems unlikely that RuBisCO degradation plays such a

POSTPRINT :

Version définitive du manuscrit publié dans / Final version of the manuscript published in :
Proteomics, 2010, 10(3), 349-368

473 major role in cambial response to Cd so as to involve about 20% of the identified
474 proteome changes. Therefore, the precise role of these proteins remains intriguing.

475 The proteomic changes described in this study, when compared with the literature, are
476 implied in other constraints as part of a generic stress pattern and do not show any Cd- or
477 even metal-stress specificity^[66,67,31,68]. This is not the case of the overexpression of DAP
478 which constitutes a putative Cd-specific response of cambial tissue

479 This study focused on young fully developed leaves, is it probable that other leaf
480 levels would exhibit nuances in their response profiles, for it is known that stress
481 response depends on the age of the tissue^[69], that cadmium affects more strongly basal
482 leaves of spinach^[4], and that some plants achieve tolerance towards metals by
483 preferential storage in organs, tissues, cells or organelles^[70,13]. We besides reported that
484 lack of compartmentalization could be linked to *P. tremula* x *P. alba* sensitivity to Cd²⁺
485^[71].

486

487 Conclusion

488 In leaves containing 84 mg Cd.kg⁻¹, the Cd toxicity principally impaired
489 photosynthesis and primary metabolism. Consequently, primary growth was reduced. The
490 resulting loss of photosynthates in all plant tissues, like cambium, partly accounts for the
491 decreased activity of these tissues. So, cambial proteome changes resulted in part from a
492 systemic toxicity, and in part from the 123 mg Cd.kg⁻¹ present inside the tissue. The
493 proteomics data presented here showed contrasted responses to Cd between leaf and
494 cambial zone.

495 It now seems important to explore whether the patterns of the proteome response of
496 the different tissues persist whatever the constraint (e.g. under drought or heat stress). If
497 so, the General Adaptation Syndrome description for plant under stress could be enriched
498 with tissue-localized markers.

POSTPRINT :

Version définitive du manuscrit publié dans / Final version of the manuscript published in :
Proteomics, 2010, 10(3), 349-368

499

References

500

501

502

503

1. Cui, Y., Zhu, Y. G., Zhai, R., Huang, Y., Qiu, Y., and Liang, J., Exposure to metal mixtures and human health impacts in a contaminated area in Nanning, China. *Environment International*. 2005, *31*, 784-790.

504

505

2. Sanita di Toppi, L. and Gabrielli, R., Response to cadmium in higher plants. *Environ exp Bot.* 1999, *41*, 105-130.

506

507

508

509

3. Cosio, C., Vollenweider, P., and Keller, C., Localization and effects of cadmium in leaves of a cadmium-tolerant willow (*Salix viminalis L.*): I. Macrolocalization and phytotoxic effects of cadmium. *Environ exp Bot.* 2006, *58*, 64-74.

510

511

512

4. Fagioni, M., D'Amici, G. M., Timperio, A. M., and Zolla, L., Proteomic analysis of multiprotein complexes in the thylakoid membrane upon cadmium treatment. *J Prot Res.* 2009, *8*, 310-326.

513

514

5. Shute, T. and Macfie, S. M., Cadmium and zinc accumulation in soybean: A threat to food safety? *Science of the Total Environment*. 2006, *371*, 63-73.

515

516

517

518

6. Unterbrunner, R., Puschenreiter, M., Sommer, P., Wieshammer, G., Tlustos, P., Zupan, M., and Wenzel, W. W., Heavy metal accumulation in trees growing on contaminated sites in Central Europe. *Environ Pollut.* 2007, *148*, 107-114.

519

520

521

522

7. Renaut, J., Bohler, S., Hausman, J.-F., Hoffmann, A. A., Sergeant, K., Nagib, A., Jolivet, Y., and Dizengremel, P., The impact of atmospheric composition on plants. A case study of ozone and poplar. *Mass Spectrom Rev.* 2008, *28*, 495-516.

523

524

525

526

8. Caruso, A., Chefdor, F., Carpin, S., Depierreux, C., Delmotte, F. M., Kahlem, G., and Morabito, D., Physiological characterization and identification of genes differentially expressed in response to drought induced by PEG 6000 in *Populus canadensis* leaves. *J Plant Physiol.* 2008, *165*, 932-941.

527

528

529

9. Robinson, B. H., Mills, T. M., Petit, D., Fung, L. E., Green, S. R., and Clothier, B. E., Natural and induced cadmium-accumulation in poplar and willow: Implications for phytoremediation. *Plant Soil.* 2000, *227*, 301-306.

530

531

10. Hall, J. L., Cellular mechanisms for heavy metal detoxification and tolerance. *J exp Bot.* 2002, *53*, 1-11.

532

533

534

535

11. Aina, R., Labra, M., Fumagalli, P., Vannini, C., Marsoni, M., Cucchi, U., Bracale, M., Sgorbati, S., and Citterio, S., Thiol-peptide level and proteomic changes in response to cadmium toxicity in *Oryza sativa* L. roots. *Environ exp Bot.* 2007, *59*, 381-392.

POSTPRINT :

Version définitive du manuscrit publié dans / Final version of the manuscript published in :
Proteomics, 2010, 10(3), 349-368

- 536 12. Sarry, J.-E., Kuhn, L., Ducruix, C., Lafaye, A., Junot, C., Hugouvieux, V., Jourdain,
537 A., Bastien, O., Fievet, J. B., Vailhen, D., Amekraz, B., Moulin, C., Ezan,
538 E., Garin, J., and Bourguignon, J., The early responses of *Arabidopsis*
539 *thaliana* cells to cadmium exposure explored by protein and metabolite
540 profiling analyses. *Proteomics*. 2006, 6, 2190-2199.
- 541 13. Fagioni, M. and Zolla, L., Does the different proteomic profile found in apical and
542 basal leaves of spinach reveal a strategy of this plant toward cadmium
543 pollution response? *J Prot Res*. 2009, 8, 2519-2529.
- 544 14. Tuomainen, M. H., Nunan, N., Lehesranta, S. J., Tervahauta, A. I., Hassinen, V. H.,
545 Schat, H., Koistinen, K. M., Auriola, S., McNicol, J., and Kärenlampi, S. O.,
546 Multivariate analysis of protein profiles of metal hyperaccumulator *Thlaspi*
547 *caerulescens* accessions. *Proteomics*. 2006, 6, 3696-3706.
- 548 15. Ahsan, N., Renaut, J., and Komatsu, S., Recent developments in the application of
549 proteomics to the analysis of plant responses to heavy metals. *Proteomics*.
550 2009, 9, 2602-2621.
- 551 16. Kieffer, P., Schröder, P., Dommes, J., Hoffmann, L., Renaut, J., and Hausman, J. F.,
552 Proteomic and enzymatic response of poplar to cadmium stress. *J
553 Proteomics*. 2009, 72, 379-396.
- 554 17. Kieffer, P., Planchon, S., Oufir, M., Ziebel, J., Dommes, J., Hoffmann, L.,
555 Hausman, J. F., and Renaut, J., Combining proteomics and metabolite
556 analyses to unravel cadmium stress-response in poplar leaves. *J Prot Res*.
557 2009, 8, 400-417.
- 558 18. Wang, W., Vinocur, B., Shoseyov, O., and Altman, A., Role of plant heat-shock
559 proteins and molecular chaperones in the abiotic stress response. *Trends
560 Plant Sci*. 2004, 9, 244-251.
- 561 19. Trovato, M., Mattioli, R., and Costantino, P., Multiple roles of proline in plant
562 stress tolerance and development. *Rendiconti Lincei*. 2008, 19, 325-346.
- 563 20. Wasternack, C., Jasmonates: an update on biosynthesis, signal transduction and
564 action in plant Stress Response, Growth and Development. *Annals of
565 Botany*. 2007, mcm079.
- 566 21. Foyer, C. H. and Noctor, G., Oxidant and antioxidant signalling in plants: a re-
567 evaluation of the concept of oxidative stress in a physiological context. *Plant
568 Cell Environ*. 2005, 28, 1056.
- 569 22. Selye, H., The General-Adaptation-Syndrome. *Ann Rev Med*. 1951, 2, 327-342.
- 570 23. Leshem, Y. Y., Kuiper, P. J. C., Erdei, L., Lurie, S., and Perl-Treves, R., Do Selye's
571 mammalian "GAS" concept and "co-stress" response exist in plants? *Ann
572 NY Acad Sci*. 1998, 851, 199-208.

POSTPRINT :

Version définitive du manuscrit publié dans / Final version of the manuscript published in :
Proteomics, 2010, 10(3), 349-368

- 573 24. Küpper, H., Parameswaran, A., Leitenmaier, B., Trtílek, M., and Šetlík, I.,
 574 Cadmium-induced inhibition of photosynthesis and long-term acclimation to
 575 cadmium stress in the hyperaccumulator *Thlaspi caerulescens*. *New Phytol.*
 576 2007, 175, 655-674.
- 577 25. Celedon, P. A. F., de Andrade, A., Meireles, K. G. X., Costa da Cruz Gallo de
 578 Carvalho, M., Gregorio Gomes Caldas, D., Moon, D. H., Carneiro, R. T.,
 579 Franceschini, L. M., Oda, S., and Labate, C. A., Proteomic analysis of the
 580 cambial region in juvenile *Eucalyptus grandis* at three ages. *Proteomics*.
 581 2007, 7, 2258-2274.
- 582 26. Gion, J.-M., Lalanne, C., Le Provost, G., Ferry-Dumazet, H., Paiva, J., Chaumeil,
 583 P., Frigerio, J.-M., Brach, J., Barré, A., de Daruvar, A., Claverol, S.,
 584 Bonneu, M., Sommerer, N., Negroni, L., and Plomion, C., The proteome of
 585 maritime pine wood forming tissue. *Proteomics*. 2005, 5, 3731-3751.
- 586 27. Lippert, D., Chowira, S., Ralph, S. G., Zhuang, J., Aeschliman, D., Ritland, C.,
 587 Ritland, K., and Bohlmann, J., Conifer defense against insects: proteome
 588 analysis of Sitka spruce (*Picea sitchensis*) bark induced by mechanical
 589 wounding or feeding by white pine weevils (*Pissodes strobi*). *Proteomics*.
 590 2007, 7, 248-270.
- 591 28. Plomion, C., Lalanne, C., Claverol, S., Kohler, A., Bogeat-Triboulot, M.-B., Barre,
 592 A., Le Provost, G., Dumazet, H., Jacob, D., Bastien, C., Dreyer, E., de
 593 Daruvar, A., Guehl, J.-M., Schmitter, J.-M., Martin, F., and Bonneau, M.,
 594 Mapping the proteome of poplar and application to the discovery of
 595 drought-stress responsive proteins. *Proteomics*. 2006, 6, 6509-6527.
- 596 29. Durand, T. C., Hausman, J.-F., Carpin, S., Albéric, P., Baillif, P., Label, P., and
 597 Morabito, D., Zinc and cadmium effects on growth and ion distribution in
 598 *Populus tremula* × *Populus alba*. *Biol Plant.* 2009, submitted.,
- 599 30. Damerval, C., De Vienne, D., Zivy, M., and Thiellement, H., Technical
 600 improvement in two-dimensional electrophoresis increase the level of
 601 genetic variation detected in wheat-seedling proteins. *Electrophoresis*. 1986,
 602 7, 52-54.
- 603 31. Bohler, S., Bagard, M., Oufir, M., Planchon, S., Hoffmann, L., Jolivet, Y.,
 604 Hausman, J.-F., Dizengremel, P., and Renaut, J., A DIGE analysis of
 605 developing poplar leaves subjected to ozone reveals major changes in
 606 carbon metabolism. *Proteomics*. 2007, 7, 1584-1599.
- 607 32. Hunter, S., Apweiler, R., Attwood, T. K., Bairoch, A., Bateman, A., Binns, D.,
 608 Bork, P., Das, U., Daugherty, L., Duquenne, L., Finn, R. D., Gough, J., Haft,
 609 D., Hulo, N., Kahn, D., Kelly, E., Laugraud, A., Letunic, I., Lonsdale, D.,
 610 Lopez, R., Madera, M., Maslen, J., McAnulla, C., McDowall, J., Mistry, J.,
 611 Mitchell, A., Mulder, N., Natale, D., Orengo, C., Quinn, A. F., Selengut, J.,
 612 D., Sigrist, C. J. A., Thimma, M., Thomas, P. D., Valentin, F., Wilson, D.,

POSTPRINT :

Version définitive du manuscrit publié dans / Final version of the manuscript published in :
Proteomics, 2010, 10(3), 349-368

- 613 Wu, C. H., and Yeats, C., InterPro: the integrative protein signature
 614 database. *Nucl Acids Res.* 2009, *37*, D211-D215.
- 615 33. Anderson, R. H. and Basta, N. T., Application of ridge regression to quantify
 616 marginal effects of collinear soil properties on phytoaccumulation of
 617 arsenic, cadmium, lead, and zinc. *Environ Toxicol Chem.* 2009, *28*, 619-
 618 628.
- 619 34. Ruttens, A., Mench, M., Colpaert, J. V., Boisson, J., Carleer, R., and Vangronsveld,
 620 J., Phytostabilization of a metal contaminated sandy soil. I: Influence of
 621 compost and/or inorganic metal immobilizing soil amendments on
 622 phytotoxicity and plant availability of metals. *Environ Pollut.* 2006, *144*,
 623 524-532.
- 624 35. Barcelo, J. and Poschenrieder, C., Plant water relations as affected by heavy metal
 625 stress: A review. *J Plant Nutr.* 1990, *13*, 1-37.
- 626 36. Chaffei, C., Pageau, K., Suzuki, A., Gouia, H., Ghorbel, M. H., and Masclaux-
 627 Daubresse, C., Cadmium toxicity induced changes in nitrogen management
 628 in *Lycopersicon esculentum* leading to a metabolic safeguard through an
 629 amino acid storage strategy. *Plant Cell Physiol.* 2004, *45*, 1681-1693.
- 630 37. Clemens, S., Toxic metal accumulation, responses to exposure and mechanisms of
 631 tolerance in plants. *Biochimie.* 2006, *88*, 1707-1719.
- 632 38. Shi, G. and Cai, Q., Photosynthetic and anatomic responses of peanut leaves to
 633 cadmium stress. *Photosynthetica.* 2008, *46*, 627-630.
- 634 39. Zhu, R., Macfie, S. M., and Ding, Z., Cadmium-induced plant stress investigated by
 635 scanning electrochemical microscopy. *J exp Bot.* 2005, *56*, 2831-2838.
- 636 40. Lindahl, M., Spetea, C., Hundal, T., Oppenheim, A. B., Adam, Z., and Andersson,
 637 B., The thylakoid FtsH protease plays a role in the light-induced turnover of
 638 the Photosystem II D1 protein. *Plant Cell.* 2000, *12*, 419-432.
- 639 41. Kieffer, P., Dommes, J., Hoffmann, L., Hausman, J.-F., and Renaut, J., Quantitative
 640 changes in protein expression of cadmium-exposed poplar plants.
 641 *Proteomics.* 2008, *8*, 2514-2530.
- 642 42. He, X. Y., Fu, S. L., Chen, W., Zhao, T. H., Xu, S., and Tuba, Z., Changes in
 643 effects of ozone exposure on growth, photosynthesis, and respiration of
 644 Ginkgo biloba in Shenyang urban area. *Photosynthetica.* 2007, *45*, 555-561.
- 645 43. Mittler, R., Abiotic stress, the field environment and stress combination. *Trends
 646 Plant Sci.* 2006, *11*, 15-19.
- 647 44. Mendoza-Cozatl, D. G., Butko, E., Springer, F., Torpey, J. W., Komives, E., Kehr,
 648 J., and Schroeder, J. I., Identification of high levels of phytochelatins,

POSTPRINT :

Version définitive du manuscrit publié dans / Final version of the manuscript published in :
Proteomics, 2010, 10(3), 349-368

- 649 glutathione and cadmium in the phloem sap of *Brassica napus*. A role for
650 thiol-peptides in the long-distance transport of cadmium and the effect of
651 cadmium on iron translocation. Plant J. 2008, 54, 249-259.
- 652 45. Semane, B., Cuypers, A., Smeets, K., Van Belleghem, F., Horemans, N., Schat, H.,
653 and Vangronsveld, J., Cadmium responses in *Arabidopsis thaliana*:
654 glutathione metabolism and antioxidative defence system. Physiol Plant.
655 2007, 129, 519-528.
- 656 46. Dixon, D. P., Cummins, I., Cole, D. J., and Edwards, R., Glutathione-mediated
657 detoxification systems in plants. Curr Opin Plant Biol. 1998, 1, 258-266.
- 658 47. Chen, J. W., Dodia, C., Feinstein, S. I., Jain, M. K., and Fisher, A. B., 1-Cys
659 peroxiredoxin, a bifunctional enzyme with glutathione peroxidase and
660 phospholipase A2 activities. J Biol Chem. 2000, 275, 28421-28427.
- 661 48. Wahid, A., Ghani, A., and Javed, F., Effect of cadmium on photosynthesis, nutrition
662 and growth of mungbean. Agronomy for Sustained Development. 2008, 28,
663 273-280.
- 664 49. Crombie, H., Chengappa, S., Jarman, C., Sidebottom, C., Grant, R., and Reid, J. G.,
665 Molecular characterisation of a xyloglucan oligosaccharide-acting α-D-
666 xylosidase from nasturtium (*Tropaeolum majus* L.) cotyledons that
667 resembles plant 'apoplastic' α-D-glucosidases. Planta. 2002, 214, 406-413.
- 668 50. Rolland, F., Baena-Gonzalez, E., and Sheen, J., Sugar sensing and signaling in
669 plants: conserved and novel mechanisms. Annu Rev Plant Biol. 2006, 57,
670 675-709.
- 671 51. Jouve, L., Hoffmann, L., and Hausman, J.-F., Polyamine, carbohydrate, and proline
672 content changes during salt stress exposure of aspen (*Populus tremula* L.):
673 involvement of oxidation and osmoregulation metabolism. Plant Biol. 2004,
674 6, 74-80.
- 675 52. Wang, J., Ji, Q., Jiang, L., Shen, S., Fan, Y., and Zhang, C., Overexpression of a
676 cytosol-localized rhamnose biosynthesis protein encoded by *Arabidopsis*
677 RHM1 gene increases rhamnose content in cell wall. Plant Phys Biochem.
678 2009, 47, 86-93.
- 679 53. Mijnsbrugge, K. V., Meyermans, H., Van Montagu, M., Bauw, G., and Boerjan,
680 W., Wood formation in poplar: identification, characterization, and seasonal
681 variation of xylem proteins. Planta. 2000, 210, 589-598.
- 682 54. Xu, S. L., Rahman, A., Baskin, T. I., and Kieber, J. J., Two Leucine-Rich Repeat
683 Receptor Kinases Mediate Signaling, Linking Cell Wall Biosynthesis and
684 ACC Synthase in *Arabidopsis*. Plant Cell. 2008, 20, 3065-3079.

POSTPRINT :

Version définitive du manuscrit publié dans / Final version of the manuscript published in :
Proteomics, 2010, 10(3), 349-368

- 685 55. Sagi, G., Katz, A., Guenoune-Gelbart, D., and Epel, B. L., Class 1 reversibly
686 glycosylated polypeptides are plasmodesmal-associated proteins delivered to
687 plasmodesmata via the Golgi apparatus. Plant Cell. 2005, 17, 1788-1800.
- 688 56. De Pino, V., Boran, M., Norambuena, L., Gonzalez, M., Reyes, F., Orellana, A.,
689 and Moreno, S., Complex formation regulates the glycosylation of the
690 reversibly glycosylated polypeptide. Planta. 2007, 226, 335-345.
- 691 57. Garnier, L., Simon-Plas, F., Thuleau, P., Agnel, J.-P., Blein, J.-P., Ranjeva, R., and
692 Montillet, J.-L., Cadmium affects tobacco cells by a series of three waves of
693 reactive oxygen species that contribute to cytotoxicity. Plant Cell Environ.
694 2006, 29, 1956-1969.
- 695 58. Kim, Y.-O., Kim, J. S., and Kang, H., Cold-inducible zinc finger-containing
696 glycine-rich RNA-binding protein contributes to the enhancement of
697 freezing tolerance in *Arabidopsis thaliana*. Plant Journal. 2005, 42, 890-900.
- 698 59. Battaglia, M., Solorzano, R., Hernandez, M., Cuellar-Ortiz, S., Garcia-Gomez, B.,
699 Marquez, J., and Covarrubias, A., Proline-rich cell wall proteins accumulate
700 in growing regions and phloem tissue in response to water deficit in
701 common bean seedlings. Planta. 2007, 225, 1121-1133.
- 702 60. Akoh, C. C., Lee, G. C., Liaw, Y. C., Huang, T. H., and Shaw, J. F., GDSL family
703 of serine esterases/lipases. Prog Lipid Res. 2004, 43, 534-552.
- 704 61. Dalrymple, B. P., Cybinski, D. H., Layton, I., McSweeney, C. S., Xue, G. P.,
705 Swadling, Y. J., and Lowry, J. B., Three *Neocallimastix patriciarum*
706 esterases associated with the degradation of complex polysaccharides are
707 members of a new family of hydrolases. Microbiology. 1997, 143, 2605-
708 2614.
- 709 62. Hong, J., Choi, H., Hwang, I., Kim, D., Kim, N., Choi, D., Kim, Y., and Hwang, B.,
710 Function of a novel GDSL-type pepper lipase gene, CaGLIP1, in disease
711 susceptibility and abiotic stress tolerance. Planta. 2008, 227, 539-558.
- 712 63. Broadley, M. R., White, P. J., Hammond, J. P., Zelko, I., and Lux, A., Zinc in
713 plants. New Phytol. 2007, 173, 677-702.
- 714 64. Kato, Y., Yamamoto, Y., Murakami, S., and Sato, F., Post-translational regulation
715 of CND41 protease activity in senescent tobacco leaves. Planta. 2005, 222,
716 643-651.
- 717 65. Goué, N., Lesage-Descauses, M.-C., Meller, E. J., Magel, E., Label, P., and
718 Sundberg, B., Microgenomic analysis reveals cell type-specific gene
719 expression patterns between ray and fusiform initials within the cambial
720 meristem of *Populus*. New Phytol. 2008, 180, 45-56.

POSTPRINT :

Version définitive du manuscrit publié dans / Final version of the manuscript published in :
Proteomics, 2010, 10(3), 349-368

- 721 66. Xiao, X., Yang, F., Zhang, S., Korpelainen, H., and Li, C., Physiological and
722 proteomic responses of two contrasting *Populus cathayana* populations to
723 drought stress. *Physiol Plant.* 2009, *136*, 150-168.
- 724 67. Renaut, J., Lutts, S., Hoffmann, L., and Hausman, J.-F., Responses of poplar to
725 chilling temperatures : proteomic and physiological aspects. *Plant Biol.*
726 2004, *6*, 81-90.
- 727 68. Alvarez, S., Berla, B. M., Sheffield, J., Cahoon, R. E., Jez, J. M., and Hicks, L. M.,
728 Comprehensive analysis of the *Brassica juncea* root proteome in response to
729 cadmium exposure by complementary proteomic approaches. *Proteomics.*
730 2009, *9*, 2419-2431.
- 731 69. Bray, Elizabeth A., Bailey-Serres, Julia, and Weretilnyk, Elizabeth.
732 Response to abiotic stresses. In: Buchanan, B., Gruissem, W., and
733 Jones, R., editors. *Biochemistry & Molecular Biology of*
734 *Plants*:American Society of Plant Physiologists; 2000 p.1158-1203.
- 735 70. Vollenweider, P., Cosio, C., and Keller, C., Localization and effects of cadmium in
736 leaves of a cadmium-tolerant willow (*Salix viminalis* L.): II.
737 Microlocalization and cellular effects of cadmium. *Environ exp Bot.* 2006,
738 *58*, 64-74.
- 739 71. Durand, T. C., Baillif, P., Albéric, P., Carpin, S., Label, P., Hausman, J.-F., and
740 Morabito, D., Cd and Zn are differentially distributed in *Populus tremula* x
741 *P. alba* exposed to metal excess. *Can J For Res.* 2010, *submitted*,
- 742
- 743

744 **CAPTION OF THE FIGURES**

745

746 **Fig. 1.** 2D-electrophoresis gel with leaf proteins of *Populus tremula x P. alba* genotype
747 717-1B4labelled by CyDye 2. Identified proteins are indicated with their respective spot
748 number.

749

750 **Fig. 2.** 2D-electrophoresis gel with cambial proteins of *Populus tremula x P. alba*
751 genotype 717-1B4 labelled by CyDye 2. Identified proteins are indicated with their
752 respective spot number.

753

754

POSTPRINT :
Version définitive du manuscrit publié dans / Final version of the manuscript published in :
Proteomics, 2010, 10(3), 349-368

755 Table 1: Differentially expressed proteins in the leaf proteome of *Populus tremula x P.alba* genotype 717-1B4 submitted during 61
 756 days to a soil containing 360 mg Cd.kg⁻¹ DW (n=4, *p<0.05, **p<0.01, ***p<0.001). The average ratio of the protein abundance was
 757 calculated between treated and control plants.

Spot number ¹	Leaf protein identifications ²	Protein score ³	Accession Number	No of peptides	Sequence coverage (%)	Cd / Ctr ratio ⁶	p value ⁷
			EST ⁴	NCBI ⁵			
Photosynthesis							
1464	RubisCO large subunit [Populus tomentosa]	283		gi 22001406	8	41	-4,3*** 0.000013
1681	RubisCO large subunit	250		gi 52001641	4	29	-4,09* 0.039
677	RubisCO large subunit	260		gi 1223722	4	57	-3,99*** 0.00083
1742	RubisCO large subunit	283		gi 9623109	4	32	-1,65* 0.039
1673	RubisCO large subunit	291		gi 30143303	6	29	-3,11** 0.003
1748	RubisCO large subunit	305		gi 60101630	5	25	-2,99** 0.0098
1750	RubisCO large subunit	113		gi 60101630	2	30	-6,02** 0.0025
1778	RubisCO large subunit [Malesherbia linearifolia]	123		gi 1771273	3	30	-2,91** 0.0032
1718	RubisCO large subunit	207		gi 1346967	3	36	-2,77* 0.019
1195	RubisCO large subunit	313		gi 57338574	6	40	-2,59* 0.014
1238	RubisCO large subunit	466		gi 60101630	7	36	-2,39* 0.022
694	RubisCO large subunit	138		gi 2149483	3	39	-2,36* 0.029
1686	RubisCO large subunit	114		gi 52001641	2	33	-2,12* 0.011
1737	Ribulose 1,5-bisphosphate carboxylase	279		gi 32442736	4	31	-3,41* 0.016
683	RubisCO large subunit [Populus alba]	172		gi 110227087	4	50	-1,58* 0.042
593	RubisCO large subunit [Populus alba]	129		gi 110227087	3	53	1,72*** 0.00032
503	Rubisco	147		gi 47680208	3	32	4,02* 0.046
648	RubisCO large subunit	300		gi 30143315	7	42	2,03* 0.012
853	Rubisco activase precursor	137		gi 3687676	2	40	-2,22** 0.01
1043	Rubisco activase B	447		gi 7960277	6	39	-1,63* 0.025
939	Rubisco activase B	168		gi 7960277	2	33	-2,2* 0.029
969	Rubisco activase, chloroplast precursor	202		gi 10720249	2	39	-1,62* 0.022
1048	Rubisco activase 1	382 (+32)	gi 52397711	gi 12620881	6	36	-1,83** 0.0092
912	RuBisCO activase	459	gi 52397711	gi 94549022	6		-2,02* 0.037
1578	Chlorophyll a/b binding protein(LhcB2) [Cicer arietinum]	219 (+70)		gi 3928140	6	69	-10,26* 0.026
1602	Chlorophyll a/b binding protein(LhcB2) [Cicer arietinum]	196 (+87)		gi 3928140	7	71	-7,67*** 0.00093
1609	Chlorophyll a/b binding protein (LhcB2)	163		gi 398599	4	18	-2,6** 0.0025
1584	Chlorophyll a/b binding protein (LhcB2)	134 (+74)		gi 398599	5	26	-2,08* 0.029
1608	LHCII type II chlorophyll a/b-binding protein [Vigna radiata]	160 (+16)		gi 9587203	6	28	-4,09**** 0.00083
1517	Light-harvesting complex II protein LhcB1 [Populus trichocarpa]	229	gi 52533657	gi 224083006	5	65	-11,02** 0.0035
1663	Chlorophyll a/b-binding protein type III (LhcA3)	133 (+117)		gi 7271947	3	26	-4,53** 0.00236
1658	Chlorophyll a/b-binding protein type III (LhcA3)	370	gi 56824867	gi 116519121	6	63	-6,11*** 0.0000043
1680	Chlorophyll-a/b binding protein LhcB3	163	gi 50059931	gi 169124051	3	70	-3,77** 0.0017
1629	LHCBl - chlorophyll binding	301		gi 15235029	3	46	-2,69*** 0.00067

POSTPRINT :
Version définitive du manuscrit publié dans / Final version of the manuscript published in :
Proteomics, 2010, 10(3), 349-368

1441	Oxygen-evolving enhancer protein 1, chloroplast precursor (OEE1)	392	gi 38580986	gi 30013657	6	51	-7.03***	0.00028
1439	Oxygen-evolving complex protein 1	250 (+60)		gi 739292	3	53	-4.42**	0.0039
1471	Oxygen-evolving enhancer protein 1, chloroplast precursor (OEE1)	198		gi 12644171	2	32	-4.81**	0.0012
1480	Oxygen-evolving enhancer protein 1	83 (+62)	gi 27410837	gi 223538464	4	54	-3.65***	0.0005
1456	Oxygen evolving enhancer protein 1 precursor	203	gi 57892741	gi 119952178	4	59	-2.75**	0.0028
1692	Oxygen-evolving enhancer protein 2, chloroplast precursor (OEE2)	169		gi 131390	3	30	-5.51***	0.00019
1653	PSBP-1 (OEE PROTEIN 2); calcium ion binding	280	gi 55735291	gi 223539254	6	49	-5.38***	0.000015
1672	Oxygen-evolving enhancer protein 2, chloroplast precursor	261	gi 55734950	gi 223539254	6	52	-4.15***	0.00067
1661	Oxygen-evolving enhancer protein 2, chloroplast precursor (OEE2)	215	gi 55735137	gi 131390	5	30	-3.73**	0.0025
1699	Oxygen-evolving enhancer protein 2, chloroplast precursor	227	gi 24099140	gi 223539254	5	62	-5.88***	0.00038
Carbohydrate metabolism								
1571	Triosephosphate isomerase, cytosolic (TIM)	304	gi 24060530	gi : 136057	6	76	1.99**	0.0026
1566	Triosephosphate isomerase, cytosolic (TIM)	180		gi 136057	5	40	2.19**	0.0039
1120	Sedoheptulose bisphosphatase	253	gi 52530247	gi 223530064	6	53	-2.48***	0.00015
1116	Sedoheptulose bisphosphatase	292	gi 52530247	gi 118175929	6	59	-1.53*	0.03
284	Transketolase 1	256 (+68)		gi 3559814	5	20	-1.61*	0.015
1127	Glyceraldehyde-3-phosphate dehydrogenase, cytosolic	185 (+157)		gi 120671	7	32	1.91***	0.00027
1124	Glyceraldehyde 3-phosphate dehydrogenase	122	gi 57892956	gi 51703306	5	81	2.07***	0.000093
1051	3-phosphoglycerate kinase [<i>Populus tremuloides</i>]	135		gi 29124969	3	46	2.45*	0.023
1275	Phosphoglycerate kinase	112 (+16)		gi 2499497	5	30	-1.75*	0.015
501	glucose-6-phosphate isomerase [<i>Solanum tuberosum</i>]	80	gi 52620161	gi 167909863	4	60	2.22**	0.0059
597	UDP-glucose pyrophosphorylase [<i>Populus tremula x P. tremuloides</i>]	226		gi 32527831	4	37	1.49**	0.0015
553	Glycosyl hydrolase family 38 protein	106	gi 56833433	gi 186510450	3	34	1.92**	0.0099
1340	Ferredoxin-NADP oxidoreductase	314		gi 170111	6	28	-1.81*	0.014
1059	Ferredoxin-NADP oxidoreductase	314 (+83)		gi 170111	8	28	-1.67*	0.017
1365	Ferredoxin-NADP oxidoreductase	190		gi 170111	3	30	-1.55*	0.04
1342	Ferredoxin-NADP oxidoreductase	257	gi 52536292	gi 4930123	6	58	-1.38*	0.015
1359	Putative ferredoxin-NADP(H) oxidoreductase	96	gi 27415025	gi 224102711	4	62	-1,5*	0.031
1332	Ferredoxin-NADP oxidoreductase	141		gi 170111	6	28	2.01**	0.003
1338	Ferredoxin-NADP oxidoreductase	156 (+83)		gi 119905	6	49	2.84***	0.00083
884	AXS2 (UDP-D-Apiose/UDP-D-Xylose synthase 2)	182	gi 27422474	gi 18390863	4	54	2.38*	0.027
1551	Acid phosphatase [<i>Glycine max</i>]	90	gi 55734561	gi 3341443	3	54	1.78*	0.014
Energy metabolism								
1598	Carbonic anhydrase	318		gi 1354515	6	63	-1.85*	0.014
1616	Carbonic anhydrase	570		gi 1354517	6	53	-1.43*	0.035
1592	Carbonic anhydrase	249		gi 1354515	4	40	-1.31*	0.049
1660	Carbonic anhydrase	118		gi 1354515	2	47	2.21**	0.018
620	ATPase beta subunit [<i>Populus tomentosa</i>] - chloroplast	354		gi 22094585	6	75	4,19***	0.00085
632	ATPase beta subunit [<i>Populus tomentosa</i>] - chloroplast	295		gi 22094585	5	75	-3,91***	0.000019
633	ATPase beta subunit [<i>Populus tomentosa</i>] - chloroplast	401 (+237)		gi 22094585	7	80	-2.02**	0.0044
594	ATPase alpha subunit [<i>Didymelis perrieri</i>] - mitochondrion	240		gi 6561625	6	38	1.83*	0.015

POSTPRINT :
Version définitive du manuscrit publié dans / Final version of the manuscript published in :
Proteomics, 2010, 10(3), 349-368

599	ATPase alpha subunit [<i>Didymelus perrieri</i>] - mitochondrion	137 (+71)		gi 6561625	4	33	2.51*	0.011
Protein metabolism & catabolism								
1290	Aminomethyltransferase, mitochondrial precursor	162		gi 3334196	2	36	-1.7*	0.028
548	D-3-phosphoglycerate dehydrogenase, putative [<i>Ricinus communis</i>]	72 (+22)	gi 23995055	gi 223542068	3	29	36,78*	0.025
435	FtsH protease 8 / ATPase/Zn dependant metallopeptidase	98		gi 42561751	4	30	-1.51*	0.014
1678	PBD1 (PROTEASOME SUBUNIT PRGB); peptidase	146		gi 15228805	2	20	-1.49*	0.028
Protein folding								
1518	Nascent polypeptide associated complex alpha chain [<i>Nicotiana benthamiana</i>]	199	gi 52502629	gi 124484511	2	60	-3,72**	0.0081
1752	Nascent polypeptide associated complex alpha chain (<i>Oryza sativa</i>)	183		gi 46575976	2	50	-5,45**	0.0024
1011	Heat shock protein 70	214		gi 48716124	3	41	-1.59**	0.0064
357	Heat shock protein 70	535 (+81)		gi 6911551	8	38	1.6*	0.014
1635	Chloroplast chaperonin 21 [<i>Vitis vinifera</i>].	188	gi 52519679	gi 50660327	5		-2.23*	0.016
427	Chaperonin, putative	81		gi 15232923	3	37	2.44	0.027
Citrate Cycle								
1200	NAD-dependent malate dehydrogenase	87 (+57)		gi 15982948	2	37	-1,84***	0.00037
1316	Malate dehydrogenase, putative [<i>Ricinus communis</i>]	79	gi 52536153	gi 223538636	3	35	-1,75**	0.0038
902	Citrate (si)-synthase [<i>Populus trichocarpa</i>]	177	gi 53783182	gi 1648926	6	33	2.11**	0.0034
903	Citrate (si)-synthase [<i>Populus trichocarpa</i>]	119		gi 1648926	2	37	1.99**	0.0091
418	Succinate dehydrogenase	168		gi 115470493	4	25	1.45*	0.046
Oxidoreductase								
936	GDP-mannose 3,5-epimerase/ NAD binding	294		gi 15241945	4	45	1.85**	0.0086
1202	Aldo/keto reductase family-like protein	121	gi 60216418	gi 23495741	5	63	-2.62**	0.0037
1061	Formate dehydrogenase	166 (+13)	gi 38593943	gi 224129102	5	51	2,08**	0.0043
1821	Peroxiredoxin type 2, putative	187	gi 52505836	gi 15231718	2	57	-2.09*	0.025
1637	1-cys peroxiredoxin [<i>Xerophyta viscosa</i>]	151		gi 19423862	2	10	16.7***	0.000013
Glutathione metabolism								
1659	Glutathione S-transferase	417	gi 55734403	gi 161347485	7	48	2.11**	0.0071
1667	Glutathione S-transferase	196	gi 24102869	gi 161347485	4	55	2.12*	0.018
Miscellaneous								
1552	Class IV chitinase [<i>Galega orientalis</i>].	285	gi 57894645	gi 33414046	3	63	1,99*	
572	Inositol-3-phosphate synthase (Myo-inositol-1-phosphate synthase)	391		gi 14548095	6	21	-1.99**	0.0082
1192	Alpha tubulin [<i>Nicotiana tabacum</i>]	224 (+74)		gi 11967906	6	38	-2.94*	0.04
1300	Potassium channel beta subunit	143 (+27)		gi 3402279	3	9	1.6**	0.0079
1756	Auxin-binding protein ABP19a precursor, putative [<i>Ricinus communis</i>]	142	gi 52530576	gi 223539406	5	14	-2.56*	0.037
225	Translation elongation factor EF-G [<i>Glycine max</i>]	354 (+47)		gi 402753	5	37	-1.64***	0.00046

Spots presenting more than one protein identification						
1736	Glutathione S-transferase + Germin-like	84	gi 51556908	29	-3,41*	0.074
1801	Plastoquinol-plastocyanin reductase	71	gi 4586598	25	-4,93**	0.0036

758

- 759 1: spot number on the master gel
 760 2: Protein obtained by blasting the EST against the NCBInr database
 761 3: MASCOT score (protein score as given by the GPS software (Applied Biosystems))
 762 4: Accession number of the EST sequence in the NCBInr database
 763 5: Accession number of the corresponding protein in the NCBInr database
 764 6: Average ratio of the protein abundance (Cadmium/Control). Positive values of ratio are given as such, negative values are given according to the following
 765 formula : given value = -1/average ratio
 766 7: p-value of Student's t-test.
 767

768
769 Table 2: Differentially expressed proteins in the cambial zone proteome of *Populus tremula x P.alba* 717-1B4 genotype after 61 days
770 on a soil containing 360 mg Cd.kg⁻¹ DW (n=4). The average ratio of the protein abundance was calculated between treated and control
771 plants.

772

Spot number ¹	Cambial protein identifications ²	Protein score ³	Accession Number	Nb of peptides	Sequence coverage (%)	Cd / Ctr ratio ⁶	p value ⁷
		EST ⁴	NCBI ⁵				
Carbon and carbohydrate metabolism							
784	Enolase1 [Zea mays]	395	gi 24075693	gi 162458207	6	81	-1.39** 0.0013
798	Enolase1 [Zea mays]	249	gi 24102975	gi 162458207	4	61	-1.38** 0.0015
816	Enolase [<i>Brassica napus</i>]	142	gi 24020181	gi 34597332	4		-1.73*** 0.00048
802	Enolase1 [Zea mays]	358		gi 162458207	4	42	-1.74*** 0.00022
800	Os0gg0136600 [<i>Oryza sativa</i> (japonica cultivar-group)]	130		gi 115466256	4	36	-2.1*** 0.00035
759	Triosephosphate isomerase-like protein [<i>Solanum tuberosum</i>].	96	gi 52505071	gi 76573375	3	33	-1.59* 0.01
752	UDP-glucose pyrophosphorylase [<i>Populus tremula x P. tremuloides</i>]	239		gi 32527831	3	19	-1.52* 0.028
744	UDP-glucose dehydrogenase [<i>Populus tremula x P. tremuloides</i>]	313		gi 6164591	6	66	-1.58** 0.0015
809	UDP-glucose dehydrogenase [<i>Populus tremula x P. tremuloides</i>]	132 (+61)	gi 57892820		4	55	-1.43** 0.0011
792	UDP-glucose dehydrogenase	151 (+59)	gi 27415980	gi 6164591	4	82	-3.47** 0.0012
851	Phosphofructokinase family protein [<i>Arabidopsis thaliana</i>]	82 (+37)	gi 27411363	gi 15238818	5	44	-2.04*** 0.0002
526	2,3-bisphosphoglycerate-independent phosphoglycerate mutase	110	gi 52493827	gi 223540739	2	59	-1.82*** 0.00036
288	Alpha-D-xylosidase [<i>Tropaeolum majus</i>]	123	gi 73928193	gi 5725356	2	23	1.53* 0.012
1892	Alpha-D-xylosidase precursor [<i>Arabidopsis thaliana</i>]	111	gi 28606907	gi 4163997	3		1.51* 0.01
390	Alpha-mannosidase [<i>Arabidopsis thaliana</i>]	113		gi 10177664	3	10	1.77** 0.0015
433	Alpha-mannosidase [<i>Arabidopsis thaliana</i>]	79		gi 10177664	2	12	1.44** 0.0085
480	RHM1/ROL1 (RHAMNOSE BIOSYNTHESIS1); UDP-glucose 4,6-dehydratase/ catalytic [<i>A. thaliana</i>]	123		gi 15218420	3	17	-1.4** 0.0029
481	RHM1/ROL1 (RHAMNOSE BIOSYNTHESIS1); UDP-glucose 4,6-dehydratase/ catalytic	106		gi 15218420	3	19	1.64** 0.001
487	RHM1/ROL1 (RHAMNOSE BIOSYNTHESIS1); UDP-glucose 4,6-dehydratase/ catalytic	130		gi 15218420	4	19	-1.8*** 0.00013
1202	Fructokinase, putative [<i>Ricinus communis</i>]	170	gi 60697528	gi 223526803	5	62	-1.9***

POSTPRINT :
Version définitive du manuscrit publié dans / Final version of the manuscript published in :
Proteomics, 2010, 10(3), 349-368

1069	Alcohol dehydrogenase [<i>Populus tremula</i>]	130	gi 52851038	2	29	2.13***	0.00052	
1070	Alcohol dehydrogenase [<i>Populus tremula</i>]	220	gi 52851054	5	74	1.62***	0.00071	
Protein metabolism								
381	Methionine synthase [<i>Solanum tuberosum</i>]	146 (+96)	gi 8439545	5	30	-2.58***	0.0009	
385	Vitamin-b12 independent methionine synthase, [<i>Populus trichocarpa</i>]	328	gi 27414927	gi 224104961	6	67	-1.98**	0.0011
383	Methionine synthase [<i>Zea mays</i>]	170	gi 17017263	5	33	-1.99**	0.0022	
391	Methionine synthase [<i>Carica papaya</i>]	138	gi 24107875	gi 151347486	3	66	-1.58**	0.0045
885	S-adenosylmethionine synthetase	98	gi 15450421	4	24	-2.02***	0.0003	
891	S-adenosylmethionine synthetase [<i>Phaseolus lunatus</i>]	170	gi 24065013	gi 1346524	2	60	-1.83*	0.018
881	S-adenosylmethionine synthetase 1 [<i>Arabidopsis thaliana</i>]	100	gi 30683070	3	34	-1.88***	0.000026	
1240	O-acetylserine (thiol)lyase [<i>Populus alba x Populus tremula</i>]	121	gi 34099833	3	34	-1.38***	0.00075	
1302	60S acidic ribosomal protein P0 [<i>Zea mays</i>]	167	gi 162460698	3	32	-1.63*	0.039	
Protein catabolism								
896	26S proteasome ATPase subunit [<i>Pisum sativum</i>]	243	gi 49175787	5	82	-1.82***	0.00016	
1555	Proteasome subunit alpha type, putative [<i>Ricinus communis</i>]	154	gi 24076896	gi 223529618	3	76	-1,49*	0.034
796	Leucine aminopeptidase, putative [<i>Ricinus communis</i>]	140	gi 73877305	gi 223531128	2	62	-1,47**	0.0037
Protein folding								
537	Protein disulfide-isomerase precursor (PDI)	387	gi 24065613	gi 11133775	5	63	-1.69*	0.012
541	Protein disulfide-isomerase precursor (PDI)	433	gi 24065613	gi 11133775	5	63	-1.99***	0.00056
1161	Protein disulfide isomerase, putative [<i>Ricinus communis</i>]	101 (+18)	gi 23994033	gi 223545789	3	65	-1,71***	0.0015
715	Calreticulin-1 [<i>Glycine max</i>]	156	gi 60214695	gi 117165712	5	47	-1.88**	0.0045
Transcription and translation factors								
892	Elongation factor 1-gamma [<i>Glycine max</i>]	116	gi 24069167	gi 18958499	2	20	-1.83***	0.00015
911	Elongation factor 1-gamma [<i>Glycine max</i>]	103	gi 18958499	2	20	-1.55*	0.012	
332	Elongation factor 1-gamma [<i>Oryza sativa Japonica Group</i>]	114	gi 24103246	gi 169244489	3	60	1.65	0.073
877	DEAD box RNA helicase [<i>Pisum sativum</i>]	105	gi 25809054	3	33	1.45**	0.0023	
920	Eukaryotic initiation factor 4A [<i>Oryza sativa (japonica cultivar-group)</i>]	156 (+51)	gi 303844	3	53	-1.85*	0.01	
1830	RNA-binding glycine-rich protein-1a [<i>Nicotiana sylvestris</i>]	118	gi 52512794	gi 469070	2	52	-1.62*	0.037
1836	Glycine-rich RNA-binding protein [<i>Euphorbia esula</i>]	126 (+26)	gi 56819713	gi 2674201	2	48	6.41**	0.0021
1838	Glycine-rich RNA-binding protein [<i>Euphorbia esula</i>]	137	gi 24008735	gi 2674201	4	50	-1.89**	0.0095
Cytoskeleton & cell wall								
772	Alpha tubulin 1 [<i>Pseudotsuga menziesii</i> var. <i>menziesii</i>]	341	gi 56481443	6	71	-1.49**	0.0045	
773	Alpha-tubulin [<i>Trifolium repens</i>]	366	gi 37789885	6	71	-1.53**	0.0042	
782	Alpha-tubulin 1 [<i>Populus tremuloides</i>]	342	gi 29124983	5	52	-1.71***	0.0009	

POSTPRINT :
Version définitive du manuscrit publié dans / Final version of the manuscript published in :
Proteomics, 2010, 10(3), 349-368

708	Beta-6 tubulin [<i>Zea mays</i>]	451	gi 162459800	8	67	-1.77***	0.00051	
695	Beta-6 tubulin [<i>Zea mays</i>]	370	gi 162462765	7	59	-1.68**	0.0017	
702	Tubulin beta-5 chain (Beta-5-tubulin)	456	gi 8928427	7	58	-1.5**	0.0026	
710	Tubulin beta-5 chain (Beta-5-tubulin)	383	gi 8928427	7	59	-1.62**	0.0036	
1319	Phenylcoumaran benzylic ether reductase [<i>Populus trichocarpa</i>]	603	gi 33453463	gi 3114901	7	84	-1.57**	0.0046
1323	Phenylcoumaran benzylic ether reductase [<i>Populus trichocarpa</i>]	122	gi 33453463	gi 224066197	5	65	-1.62*	0.03
1340	Phenylcoumaran benzylic ether reductase [<i>Populus trichocarpa</i>]	415	gi 33453463	gi 224066197	5	56	-1.67*	0.012
1168	Reversibly glycosylated polypeptide	112 (+38)	gi 23978092	gi 2317729	2	11	-2.72***	0.000046
1187	Reversibly glycosylated polypeptide-1	170	gi 57894464	gi 2317729	2	76	-3.93***	0.000017
1317	Leucine rich repeat protein [<i>Populus tremula</i>]	134 (+26)	gi 33451847	gi 190897438	4	52	-1.6***	0.00065
977	Actin [<i>Stevia rebaudiana</i>]	133		gi 23955912	3	58	2.15***	0.00048
990	Actin [<i>Gossypium hirsutum</i>]	650		gi 32186906	8	77	-1.54**	0.0024
1057	Putative proline-rich protein [<i>Oryza sativa Japonica Group</i>]	193	gi 38594177	gi 14209541	2	16	-2.13*	0.027
926	Putative proline-rich protein [<i>Oryza sativa Japonica Group</i>]	83 (+46)	gi 38594177	gi 14209541	3	22	2.08**	0.0094
1324	Cinnamoyl-CoA reductase [<i>Jatropha curcas</i>]	247	gi 73869335	gi 239909311	5	27	-1.46*	0.02
Stress response - defense								
1179	Cupin family protein	140	gi 24106291	gi 15226926	6	30	-1.54***	0.00016
Citrate Cycle								
1268	NAD-dependent malate dehydrogenase [<i>Prunus persica</i>]	157	gi 52521122	gi 15982948	4	33	-1.41**	0.0037
1290	Malate dehydrogenase precursor [<i>Medicago sativa</i>]	132	gi 24062191	gi 2827080	3	54	-1.58*	0.036
1336	Malate dehydrogenase [<i>Glycine max</i>]	133	gi 73871484	gi 5929964	5	47	-1.61**	0.0062
Oxidoreductase								
1137	Peroxidase [<i>Nicotiana tabacum</i>]	147	gi 57894628	gi 14031049	4	42	2.93*	0.015
Glutathione metabolism								
1657	Glutathione-s-transferase theta, gst, putative [<i>Ricinus communis</i>]	120	gi 24100781	gi 223551315	3	57	1,66*	0.027
908	6-phosphogluconate dehydrogenase, putative [<i>Ricinus communis</i>]	146 (+32)	gi 50069101	gi 223529624	4	70	-1.54***	0.00033
909	6-phosphogluconate dehydrogenase family protein	149 (+39)	gi 50069101	gi 223529624	3	70	-1.51**	0.0012
Lipid metabolism								
1059	Acetylcholinesterase [<i>Macroptilium atropurpureum</i>]	128	gi 24064109	gi 168274274	6	38	1.46**	0.0029
1064	Acetylcholinesterase [<i>Macroptilium atropurpureum</i>]	212	gi 24064109	gi 168274274	5	38	1.59***	0.00077
1066	Acetylcholinesterase [<i>Macroptilium atropurpureum</i>]	323	gi 24064109	gi 168274274	5	39	1.89***	0.00019
572	GD\$L-motif lipase/hydrolase family protein [<i>Arabidopsis thaliana</i>]	227	gi 38594604	gi 15242458	2	33	-1.73*	0.023

POSTPRINT :
Version définitive du manuscrit publié dans / Final version of the manuscript published in :
Proteomics, 2010, 10(3), 349-368

576	GDSL-motif lipase/hydrolase family protein [<i>Arabidopsis thaliana</i>]	218	gi 23976058	gi 21553940	3	42	-1.63**	0.0042
DNA-binding aspartyl peptidase								
1140	Aspartyl protease family protein [<i>Arabidopsis thaliana</i>]	92	gi 38572690	gi 18412482	2	17	-1.66***	0.00027
913	Aspartyl protease family protein [<i>Arabidopsis thaliana</i>]	228	gi 33184151	gi 15232503	5	30	-1.46**	0.0037
996	Aspartyl protease family protein [<i>Arabidopsis thaliana</i>]	191	gi 33450735	gi 15232503	5	48	-1.64*	0.01
1157	Aspartyl protease family protein [<i>Arabidopsis thaliana</i>]	93	gi 38572403	gi 15238250	2	25	-1.34*	0.016
1146	Aspartyl protease family protein [<i>Arabidopsis thaliana</i>]	201	gi 23994041	gi 15238250	3	44	2.15***	0.00015
398	Aspartyl protease family protein [<i>Arabidopsis thaliana</i>]	148	gi 33453642	gi 15232503	5	52	5.05*	0.041
1488	Aspartyl protease family protein [<i>Arabidopsis thaliana</i>]	78 (+19)	gi 52514491	gi 15232503	4	27	2.59*	0.026
1495	Aspartyl protease family protein [<i>Arabidopsis thaliana</i>]	120	gi 27421141	gi 15232503	4	24	2.94***	0.00063
1106	41 kD chloroplast nucleoid DNA binding protein (CND41)	133	gi 23994041	gi 24430421	3	31	1.58***	0.00021
1115	Nucleoid DNA-binding protein cnd41-like protein	153	gi 38572403	gi 110740049	2	30	1.78***	0.00033
1206	Nucleoid DNA-binding protein cnd41-like protein [<i>A. thaliana</i>]	171	gi 38572403	gi 110740049	3	26	1.67*	0.012
1142	Nucleoid DNA-binding protein cnd41-like protein	226	gi 23989413	gi 8979711	2	75	2.13***	0.00029
1148	Nucleoid DNA-binding protein cnd41-like protein	113 (+71)	gi 38572403	gi 110740049	4	30	1.85**	0.0076
1149	Nucleoid DNA-binding protein cnd41-like protein	170	gi 38572403	gi 110740049	2	30	2.09**	0.0048
1169	Nucleoid DNA-binding protein cnd41-like protein	202	gi 23989413	gi 8979711	2	59	2.01**	0.0058
1177	Nucleoid DNA-binding protein cnd41-like protein	163	gi 38572403	gi 110740049	3	26	1.7*	0.04
Nucleotides metabolism								
1129	Putative adenosine kinase [<i>Populus alba x Populus tremula</i>]	66 (+54)		gi 41350585	3	55	-1.34**	0.0071
1135	Putative adenosine kinase [<i>Populus alba x Populus tremula</i>]	129		gi 41350585	3	56	-1.41**	0.0023
Miscellaneous								
1375	Putative beta-subunit of K+ channels [<i>Solanum tuberosum</i>]	180 (+32)	gi 57892112	gi 223542738	4	51	-1.69**	0.0014
1376	potassium channel beta, putative [<i>Ricinus communis</i>].	118 (+14)	gi 57892112	gi 223542738	3	51	-1.78**	0.0012
1492	Phi-1 [<i>Nicotiana tabacum</i>]	120 (+36)	gi 18014334	gi 3759184	3	59	1.99*	0.035
491	Vacuolar ATP synthase catalytic subunit A (V-ATPase subunit A)	306		gi 137460	6	55	-1.8***	0.00022
519	Vacuolar proton pump subunit alpha	220	gi 56834889	gi 137460	6	61	-1.48**	0.0028
1411	predicted protein [<i>Populus trichocarpa</i>]	150	gi 90190382	gi 224144967	3	43	-1.64*	0.012
Spots presenting more than one protein identification								
880	Eukaryotic initiation factor 4A + predicted protein	115		gi 303844			2.69***	0.00077
1112	aspartyl protease family protein + acid alpha galactosidase 1	116	gi 23989413	gi 8979711			2.58***	0.000013
1122	Glutamine synthetase + Unidentified	116		gi 37956277			-1.43**	0.0067

POSTPRINT :
Version définitive du manuscrit publié dans / Final version of the manuscript published in :
Proteomics, 2010, 10(3), 349-368

1118	Alcohol dehydrogenase [<i>Populus tremula</i>] + Aspartic proteinase nepenthesin-2 precursor, putative	82	gi 52851028	2,64**	0.003
1236	Aspartyl protease family protein + glycosylated protein	88	gi 38572690	-1.89**	0.0012
785	Adenosylhomocysteinase + Enolase + 20S proteasome subunit alpha-1	98	gi 60206618	-2.51**	0.0023
796	Glutamate decarboxylase + leucine aminopeptidase, putative	80 (+67)	gi 38581604	-1.47**	0.0037

773

774 1: spot number on the master gel

775 2: Protein obtained by blasting the EST against the NCBI nr database

776 3: MASCOT score (protein score as given by the GPS software (Applied Biosystems))

777 4: Accession number of the EST sequence in the NCBI nr database

778 5: Accession number of the corresponding protein in the NCBI nr database

779 6: Average ratio of the protein abundance (Cadmium/control). Positive values of ratio are given as such, negative values are given according to the following
780 formula : given value = -1/average ratio

781

782 Table 3 : Effect of 61 days of exposure to 360 mg Cd.kg⁻¹ SDW on different
 783 physiological parameters of *Populus tremula* x *P. alba*, genotype 717-1B4.

784

Physiological parameter	Effect of Cd treatment
Stem height	-64%
Radial growth	-95%
CO ₂ assimilation	-94%
Stomatal conductance	-56%
Cd ²⁺ content in leaves	84.0 mg.kg ⁻¹
Cd ²⁺ content in cambial zone	123 mg.kg ⁻¹
Zn ²⁺ content in leaves	+127%
Mg ²⁺ content in leaves	+91%
Ca ²⁺ in leaves	+49%
K ⁺ content in leaves	+132%
K ⁺ content in cutting	-48%

785

786 Table 4 : Summary of the principle proteome changes in the leaf and in the cambial zone
787 of *Populus tremula x P.alba*, genotype 717-1B4 exposed 61 days to 360 mg Cd.kg⁻¹ SDW.

Metabolic functions	Leaf	Cambial zone
Photosynthesis	3↑ (593, 503, 648) 41↓ (e.g. 1464, 1043)	0 0
Carbon and carbohydrate metabolism	12↑ (e.g. 501, 1127, 1571) 9↓ (e.g. 284, 1120, 1200)	7↑ (e.g. 288, 1892, 390, 481, 1070) 15↓ (e.g. 480, 802, 851)
Energy metabolism	3↑ (1660, 594, 599) 6↓ (620, 632, 633, 1598, 1616, 1592)	0 0
Protein metabolism	1↑ (548) 1↓ (1290)	0 8↓ (e.g. 381, 885, 1302, 1240)
Protein catabolism	0 2↓ (1678, 435)	0 3↓ (796, 896, 1555)
Protein folding	1↑ (357) 4↓ (1011, 1635, 1518, 1752)	0 4↓ (537, 541, 715, 1161)
Transcription & translation factors	0 1↓ (225)	2↑ (1836, 877) 6↓ (332, 920, 892, 911, 1830, 1838)
Cytoskeleton & cell wall	0 1↓ (1192)	2↑ (926, 977) 16↓ (e.g. 772, 1168, 990)
Stress Response – defense	1↑ (1552) 0	0 1↓ (1179)
Citrate Cycle	3↑ (418, 902, 903) 2↓ (1200, 1316)	0 3↓ (1268, 1290, 1336)
Oxidoreduction	3↑ (1061, 936, 1637) 2↓ (1202, 1821)	1↑ (1137) 0
Glutathione metabolism	2↑ (1659, 1667) 0	2↑ (1657, 1744) 2↓ (908, 909)
Lipid metabolism	0 0	3↑ (1064, 1066, 1059) 2↓ (572, 576)
DNA-binding Aspartyl Peptidase	0 0	4↑ (1140, 913, 996, 1157) 12↓ (e.g. 1146, 1106, 1169)
Nucleotide metabolism	0 0	0 2↓ (1129, 1135)

788
789

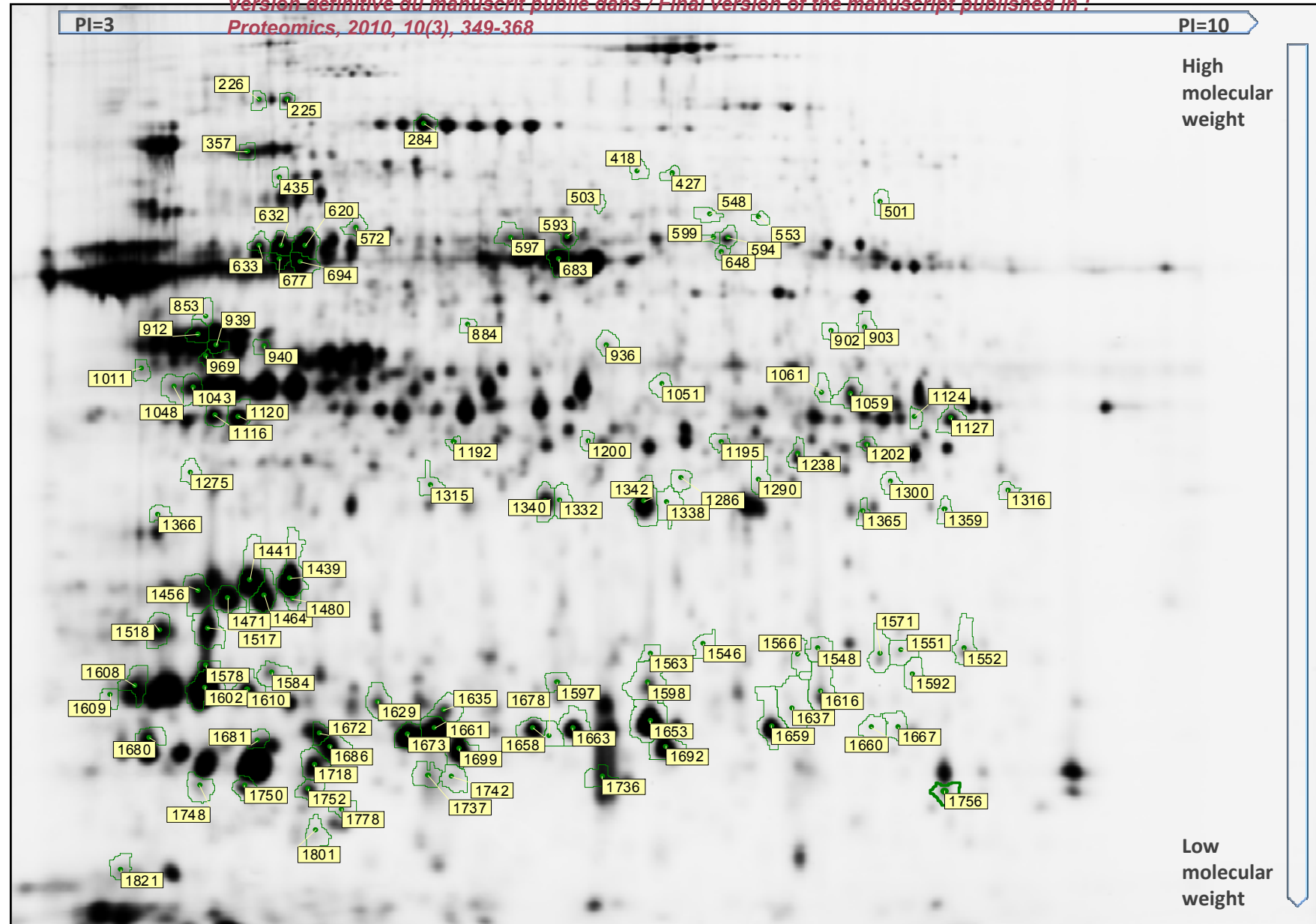


Figure 1. 2D-electrophoresis gel with Leaf proteins of *Populus tremula x P. alba* genotype 717-1B4 colored by CyDye 2. Identified proteins are labelled with their respective spot number.

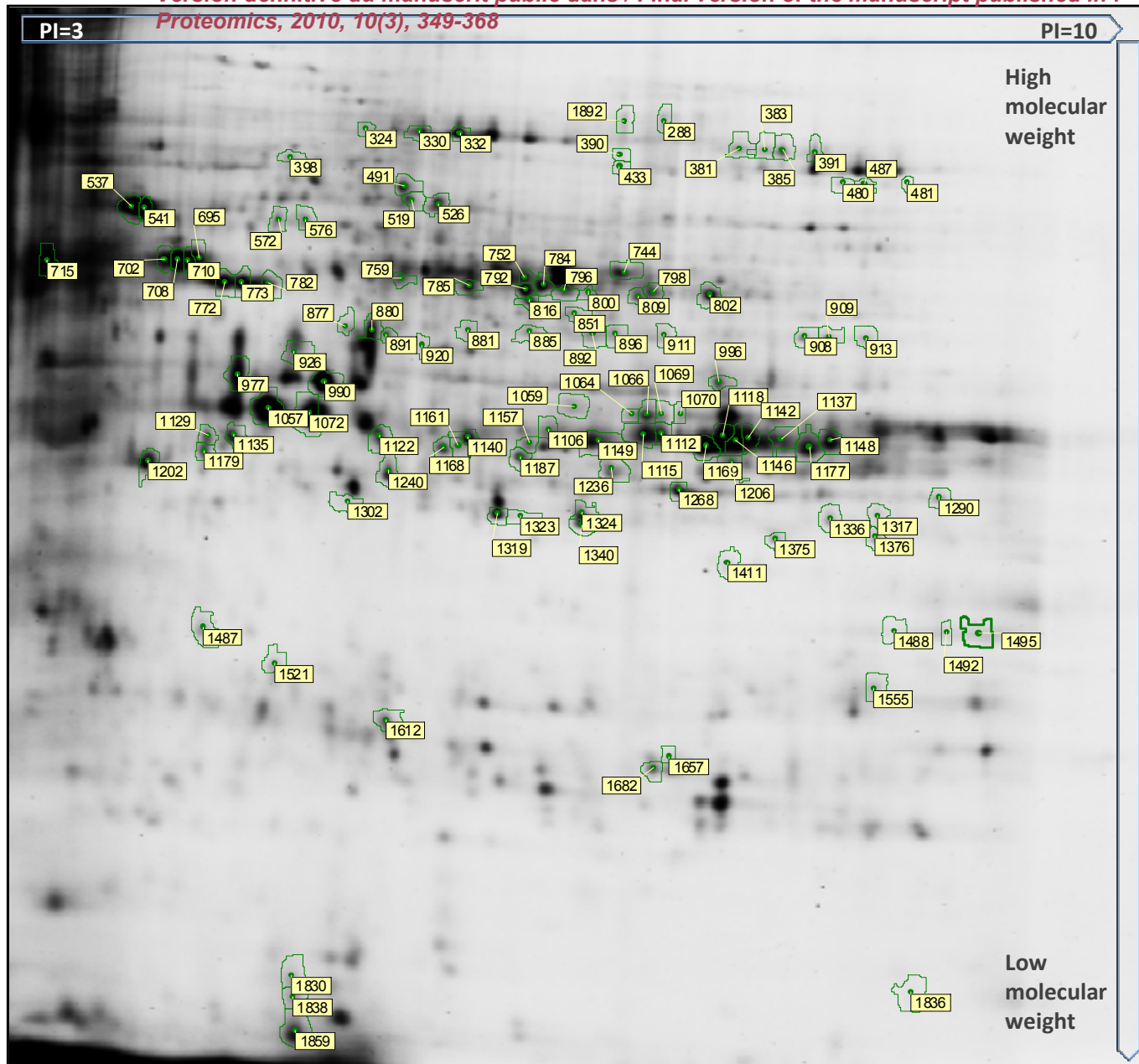


Figure 2. 2D-electrophoresis gel with **Cambial** proteins of *Populus tremula x P. alba* genotype 717-1B4 colored by CyDye 2. Identified proteins are labelled with their respective spot number.

Manuscrit d'auteur / Author manuscript

Manuscrit d'auteur / Author manuscript

Manuscrit d'auteur / Author manuscript